Water Science & Technology

IWA PUBLISHING

Water Science & Technology Vol 88 No 6, 1518 doi: 10.2166/wst.2023.280

An integrated approach to remove endocrine-disrupting chemicals bisphenol and its analogues from the aqueous environment: a review

Monica A. V., Anbalagan K.* and Becky Miriyam I.

Department of Chemical Engineering, SRM Institute of Science and Technology, Kattankulathur, Tamil Nadu 603 203, India
*Corresponding author. E-mail: anbalagk@srmist.edu.in

ABSTRACT

Bisphenol A (BPA) is a well-known endocrine-disrupting chemical (EDC) used as a plastic enhancer in producing polycarbonate resins to manufacture hard plastics. Due to strict limitations on the manufacturing and utilization of BPA, several bisphenol substitutes, bisphenol F (BPF), bisphenol S (BPS), and bisphenol AF (BPAF), have been developed to replace it in various applications. Because of their widespread use in food containers, infant bottles, and reusable water bottles, bisphenols (BPs) have been identified in different environmental circumstances, including drinking water, seawater, industrial effluent, and endocrine systems such as human blood, urine, and breast milk. However, locating and analyzing them in different conditions has proven to be challenging. Therefore, there is a need to reduce the prevalence of BPs in the environment. The significance of advanced treatment options for treating and eliminating BPA and its alternatives from water bodies are reviewed. Also, the research gaps and future scopes are discussed in this review article. According to the literature survey, adsorption and photocatalytic degradation provide synergistic benefits for environmental challenges because of their substantial adsorption Q5 capacity, high oxidation capability, and low cost compared to alternative individual treatment options.

Key words: adsorption, endocrine disruptor, photocatalytic degradation, synergetic, treatment technology, wastewater

HIGHLIGHTS

- The occurrence of bisphenols in aquatic systems has been addressed.
- The aggressive impact of endocrine-disrupting chemicals in the environmental matrices is outlined.
- The pollutant's sustainability and structural characteristics are analyzed.
- The cost-effective treatment strategies for simultaneous BPs reduction are discussed.
- The significances of BPs on the integrated treatment approach are detailed.

GRAPHICAL ABSTRACT

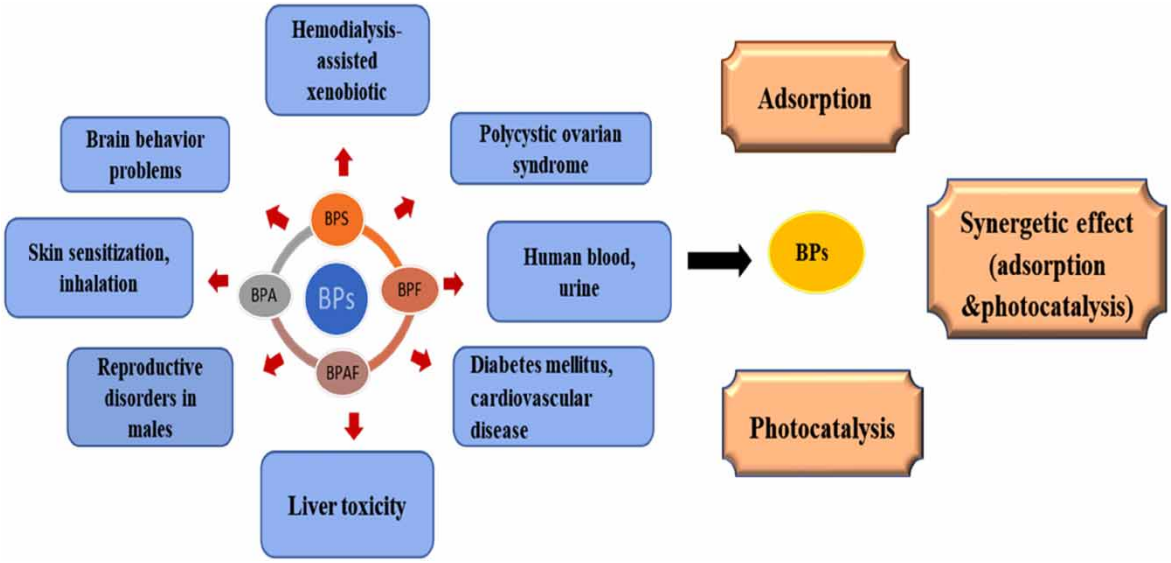

1. INTRODUCTION

Water pollution is a primary environmental concern, with a wide range of pollutants detected in aquatic environments at ng/L to g/L levels (Chen *et al.* 2006). Every year, around 1.2 million people die due to water contamination. Significant water pollution sources include household garbage, industrial development, pesticides and chemical fertilizers, plastics, polythene bags, domestic sewage from urbanization, and a weak management system. About 80% of sewage produced by humans that is not cleaned ends up in rivers or the ocean (Luyckx *et al.* 2021). According to the statistics, plastics are one of the most common pollutants discharged into the environmental matrix, primarily on land, and is a significant concern. Between the years 1950 and 2015, 8.3 billion tons of plastic products were produced, but only 6.3 billion tons of plastic waste was generated. Hardly 9% of the waste was recycled, while the remaining 12% was burned, either with or without energy recovery (Rhodes 2018). Chemicals such as phosgene and dioxides are released into the environment when plastics are incinerated, posing a hazard to the ecosystem (Rajmohan *et al.* 2019). Therefore, the interaction between illegally discarded plastic and the ecosystem provides substantial health concerns, including ingestion, inhalation, and epidermal sorption (Lusher *et al.* 2015). Over 60% of this untreated plastic waste is estimated to be deposited into the environment and landfill, with a minimum of 10% entering the oceans (Lechthaler *et al.* 2020b). In 2018, the world produced 359 million tons of plastics, with approximately 13 million tons of that ending up in aquatic environments, resulting in marine plastic pollution (MPP), which has reached epidemic proportions and has been proven to impact living creatures, human health, and economic sectors such as tourism, aquaculture, and navigation (Aretoulaki *et al.* 2020). Plastics may play a key role in human existence because of their low price and wide range of applications to maintain stability and prolonged product lifetime. Notably, personal protective equipment (PPE), especially face masks, have been widely utilized by humans to protect them from COVID-19, which is found in the environment and persists for long periods of exposure in aqueous systems and soil. According to these projections, the demand for plastic goods is expected to increase industrial output by 600 million tons by 2025 and one billion tonnes by 2050 (Jang *et al.* 2020). Despite their numerous applications, plastic waste materials might not be permissible below 25 °C, but they will surely leach into waterbodies when they reach above room temperature. This implies that microwaving leftover meals in a plastic container may expose you to an even higher concentration of potentially hazardous chemicals (Schiffmann 2017). In soil, it takes longer to disintegrate and remains in the environment for an extended period. Furthermore, several organic pollutants have been found in the ocean as plastic debris, as well as in sewage sludge and recovered effluents where they eventually accumulate in aquatic systems (Fotopoulou & Karapanagioti 2019). These plastic wastes account for 60–95% of all marine litter, from surface waters to deep-sea sediments (Lechthaler *et al.* 2020a) and into food chains (Huerta Lwanga *et al.* 2017), which implies that it is crucial for protecting ocean health and the endocrine systems.

1.1. Origin of plastic additives

Plastics are designed by polymerizing monomers and other components such as plastic additives (Okan *et al.* 2019). Additives are chemical substances that are added to a plastic polymer to offer desired qualities or to assist in plastic production and that are intentionally added during the manufacturing process to improve the performance of plastic products in terms of resistance to ozone, temperature, light radiation, mould, bacteria, and moisture, as well as mechanical, thermal, and electrical resistance (Gunaalan *et al.* 2020). Chemical additives like toxic BPA, phthalates, and brominated flame retardants, which are frequently used in the processing of plastics, also induce endocrine disruption when ingested or inhaled and seem to be present in household products and food packaging materials (Thompson *et al.* 2009). Most of these chemicals are not chemically bound. Therefore, they can leach out of materials at certain temperatures thus providing an increasingly emerging contaminant threat to marine organisms due to plastic deposition on land and ocean disintegration (Hermabessiere *et al.* 2017).

Plastic longevity estimates range from hundreds to millions of years based on the physical and chemical characteristics of the polymer materials. However, this is expected to be significantly enhanced at depths where oxygen levels are low, and light is non-existent (Barnes *et al.* 2009), leading to a loss of structural stability (Biber *et al.* 2019). Wind speeds, current flow, shoreline nature, and human influences such as urban centres and shipping routes all contribute to the spread of plastic debris in the sea (Born & Brüll 2022). Another key aspect of the process for the fragmentation of plastic debris is photodegradation produced by sunlight. UV radiation from the sun induces oxidation of the polymer chain, which leads to chemical bond disruption (Yousif & Haddad 2013). The plastic polymer materials are categorized based on their sizes, with large plastic most likely disintegrating into macroplastics (tiny plastic debris) with a size of 5–10 mm, microplastics with a size range <5 mm, nanoplastics with a size range from 1 to1 mm (Peng *et al.* 2020) and macroplastics with greater than 5 mm (Lebreton *et al.* 2019). With the finding of these materials, microplastics derived from the macroplastics have been discovered in the marine environment and they gained much attention because they can enter the environment through wastewater, storms, leaching, and natural disasters, which can transport materials of all types, including plastics, into the ocean waters (Schmaltz *et al.* 2020). Primarily microplastics are present in various packaging plastics, bottling plastic material (particularly bottled water), food processing containers (Aragaw 2021), as well as pharmaceuticals and personal care items (Cheung & Fok 2017). One of the most frequently discussed types of primary microplastics is the scrubber, which is present in exfoliating hand cleansers and cosmetic scrubs easily absorbed by human bodies. Over a thousand plastic microbeads are found in each daily-used personal care product, including toothpaste and other things (Mhiret Gela & Aragaw 2022). This subsequently became a part of a discharge from residential wastes and sewage. Secondary microplastics are generated in the environment due to plastic fragmentation caused by various physiological, bio, and chemical methods that reduce plastic stability (Debroy *et al.* 2022).

The physical structure of microplastic is minute in size, so it can be easily trapped or ingested by ocean species, which shows that it could be utilized to chemically transmit pollutants to the food supply chain and marine life (Li *et al.* 2016). It is well-accepted that marine aquatic species are exposed to plastic-related substances in greater quantities due to microplastics. Several synthetic chemicals released into the natural world were once considered relatively harmless, but researchers gradually became aware of their negative impacts on the environment and human health (Fang *et al.* 2019). Some of chemical compounds may be restricted or banned, and alternative counterparts frequently replace them. For example, BPA is a commonly utilized manufacturing chemical that acts as an endocrine disruptor in the environment. It is widely used in manufacturing products like polycarbonate polymers, adhesives, and surface coating for the lining of metallic food and beverage cans (Cooper *et al.* 2011). There is widespread awareness about the potentially hazardous effects of BPA leaching into meals and beverages and crossing the permissible limits from food packaging and storing containers, owing to the regulatory pressure, and it affects human endocrine systems. BPA is being assessed by the European Chemicals Agency (ECHA) to be identified, categorized, and used by the Registration, Evaluation, Authorization, and Restriction of Chemicals (REACH) regulation. All consumer goods supplied in the European Union must comply with the REACH regulation, which limits the use of chemicals and heavy metals. BPA was added to the ECHA's authorization list as a substance of very high concern due to its impact on human endocrine function. Since January 2020, its use in thermal paper has been limited. Just a small quantity of BPA (0.05 mg/kg) is permitted to leach from products intended for use in food contact materials. All food packaging, containers, and BPA utensils are prohibited in France. According to the Toy Safety Directive (TSD), 0.04 mg/L of BPA is the migration limit for BPA in toys (Brandsma *et al.* 2022). Based on the findings of the expert panel on food contact materials,

enzymes, and processing aids, CEP panel's reevaluation of the health risks of BPA, the European Food Safety Authority (EFSA) published a draught opinion on December 5, 2021, proposing a reduction in the tolerable daily intake (TDI) of BPA from 4 g/kg/bw/day to 0.04 ng/kg/bw/day; this is the updated assessment by 2022 (Eaton *et al.* 2022).

BPA is a class comprising anthropogenic chemicals made up of two phenolic rings joined by a bridging carbon or other chemical structure. It is employed as an intermediate for synthesizing 8 billion pounds of epoxy resins and polycarbonate polymers each year. Restricting BPA manufacturing and use has led to the development of BPs analogues such as BPS, BPF, BPE, and BPAF, as BPA substitutes for industrial applications (Yang *et al.* 2014). The synthesis of BPA and its analogues BPAF, BPF, and BPS includes a phenol condensation process with the appropriate solvent and catalyst like acetone, hexafluoroacetone, formaldehyde, and sulphur trioxide, respectively (Vasiljevic & Harner 2021). According to research, analogous chemicals have been identified in several environmental assemblages, such as indoor dust, sediments, fresh and ocean water, and sewage effluent at levels equal to or higher than that of BPA in the atmosphere (Chen *et al.* 2016a).

1.2. BPs impact on the environment

BPA was first synthesized in 1891, and its widespread industrial application began in the 1950s as a tool for producing epoxy resins and polycarbonates. BPA-containing epoxy resins are additionally utilized in materials, including bottle caps, water supply pipelines, and food containers. It can penetrate into packaged foods due to thermal processing during manufacturing, raising food safety issues (Tzatzarakis *et al.* 2017). Furthermore, it is used in materials that come into contact with food and in fabricating currency notes, thermal printing papers, compact discs, powder paints, and adhesives. These substances might build up in the environment because it is unfavourable for biodegradability (Tajik *et al.* 2020). As a result, there has been an increasing awareness in recent years of the possible detrimental effects on humans and animals from exposure to endocrine-disrupting chemicals (EDCs) (Gore *et al.* 2015). EDCs are chemicals that interfere with the action of hormones within the human body causing diseases. Some significant impacts of EDCs in humans are reproductive system issues, hypothyroidism, stroke, cancers, and obesity. Regarding vitellogenin and hatchability levels, the reproductive system of wildlife may be impacted (Kasonga *et al.* 2021). BPA is one of the typical EDCs, according to toxicology research, which replicates oestrogen's activity. Also, it is linked with an increased risk of all-cause mortality, cardiovascular illness, and high blood pressure in both experimental and epidemiological research (Moon *et al.* 2021). Also, there is a growing concern about the manufacturing and use of BPA analogues due to their disruptive effects and ecological implications.

BPA is naturally susceptible to entering the environment (Fromme *et al.* 2002), with quantities from 0.0005 to 0.41 mg/L in surface water, 0.018 to 0.702 mg/L in sewage effluents, 0.01 to 0.19 mg/kg in sediments, and 0.004 to 1.363 mg/g in sewage sludge, according to measurements. It is also found in tap water samples, ranging from 3.5 to 59.8 ng/L (Santhi *et al.* 2012). BPs are major ecological contaminants in municipal wastewater (Wang *et al.* 2019). Using an LC-MS analyzer, Chiriac *et al.* (2021) found the presence of BPs (BPA, BPB, BPC, BPE, BPF, and BPS) in influent, effluent, and surface water. The total number of analytes found in influent samples ranged from 1,337 to 16,118 ng/L, while in effluent samples it was 15–96 ng/L). In surface water, the total chemical concentration ranged from 34 to 240 ng/L. As previously stated, comparing three decades has revealed that BP contamination in the aqueous system has increased parts per million (PPM) mg/L to parts per billion (PPB) ng/L, indicating that BP levels in the aquatic system are increasing at an alarming rate year after year.

The ability of BPs to disrupt the endocrine system has also stimulated research into the consequences of prolonged exposure to male and female hormone levels, insulin levels, and hormonal imbalances (Bousoumah *et al.* 2021). Furthermore, it was noted that elevated BPA levels could have negative consequences, most notably on reproductive capacities such as female fertility, male low sperm count, quality, and changes in sex hormone concentrations (Wu *et al.* 2018). BPA was also detected in significant proportions in mother milk samples, with an average of 34.18 ng/mL, according to de Siqueira *et al.* (2023). Also, mothers' BPA concentrations were enhanced by consuming meals in plastic packaging, particularly after the plastic materials were warmed. The typical weekly consumption of BPA among nursing newborns was 19.5 g/kg/day, and the 95th percent of body weight consumed was 28.5 g/kg/day, exceeding the extreme normal amount recommended by the European Council for Food Standards (ECFS). This shows an elevated level of BPA in women's breastmilk, which could be attributed to using plastic containers as food/drink packaging. Akgül *et al.* (2019) also reported that human urine and blood frequently contain BPA, indicating a high exposure to these chemicals. The Food and Drug Administration (FDA) prohibited the use of BPA in children's sippy cups and baby bottles. BPS has overtaken BPA as the most popular alternative in North America, Asia, and Europe (Chen *et al.* 2016b). BPS is structurally similar to BPA due to including a sulphonyl ring between two

phenolic sites. BPS appears to behave similarly to EDCs, by utilizing the same metabolic disposal pathway and exhibiting oestrogenic characteristics. Shortly after BPA rules were strengthened, statistical studies discovered that average BPS consumption was roughly 0.009 g/kg/day. In parallel with its expanding use as an industrial plasticizer, BPS exposure has increased. The European Chemical Association (ECA) estimates that 10,000 million metric tons of BPS are produced and imported in Europe annually. According to research, BPS is detected in biological fluids with 97% accuracy in the US and 100% in Japan. Several in-vitro studies comparing BPS, BPF, and BPAF to BPA revealed that they have comparable or even stronger estrogenic effects (Jin *et al.* 2018). As a result, BPS and BPF were found in the abiotic environment and bodily fluids in similar concentrations but slightly lower than BPA. The average daily intake of BPs from breast milk was 531 ng/kg/day in BPA, 53 ng/kg/day for BPS, and 24–27 ng/kg/day for BPAF. BPA and its analogues in municipal wastewater are important sources of environmental contamination. BPs are more persistent in sediments ($t^{1/2} = 135$–$1{,}621$ days) than in soil ($t^{1/2} = 30$–360 days) or water ($t^{1/2} = 15$–180 days).

Because of the widespread production and high toxicity of BPs, researchers have been looking into effective methods for removing BPs from the environment for a long time, utilizing various treatment technologies made of sustainable materials. Several methods, including adsorption, photocatalytic degradation, membrane separation, and electrochemical procedures, have been developed to remove BPs from water and wastewater. Adsorption and photocatalytic degradation are advantageous to other methods due to their simple design, low investment, startup costs, and land requirement. This review article provides a detailed overview of the adsorption, photocatalytic degradation, and synergistic effects of the two techniques on different types of BPs.

1.3. Physio-chemical properties of bisphenol and its analogues

BPs are colourless solids that are soluble in most major organic solvents but have a very low solubility in water. The ability of BPs to move, transform, and spread in the environment is indicated by their octanol–water partition coefficient (log K_{ow}) value. Low K_{ow} values are thought to be highly hydrophilic, which means they have high water solubility and a low adsorption coefficient (K_{oc} values). A common bioconcentration factor in aquatic species and the acid dissociation constant (pKa) show whether a compound will be protonated or deprotonated based on the correlation between the (pKa) of a mixture and the pH of a solution. The mixture will be protonated if the pH is lower than the pKa. The combination will deprotonate if the pH exceeds the pKa (Lintelmann *et al.* 2003). Table 1 displays physiochemical data of octanol–water partition coefficient (Log $K_{o/w}$), acid dissociation constant (pKa), and some physical-chemical properties of BPs.

2. BISPHENOL REMOVAL METHODS

Several treatment strategies have traditionally been used for the removal of endocrine-disrupting substances. The most promising treatment processes are adsorption, photocatalytic degradation, electrochemical, and membrane separation. Adsorption is regarded as one of the most efficient contaminant removal techniques due to its many advantages including ease of operation, low investment in terms of both initial costs and a wide variety of adsorbents that are appropriate for pollutant removal; the only consequence is the need for adsorbent regeneration (Blinová & Sirotiak 2021). A photocatalytic approach has the advantage of removing both metal ions and organic contaminants simultaneously at the same time. However, low visible light utilization, rapid charge recombination, and the limited ability of photo-generated electrons and holes to migrate are some limitations of current photocatalytic systems that limit their industrial applications. As a result, noble metals, transition metals, nonmetals, and metalloids (graphene, carbon nanotubes, and carbon quantum dots) are doped into the photocatalyst as co-catalysts to improve photodegradation performance (Sadegh & Ali 2018). Electrochemical oxidation does have a few

Table 1 | Physical and chemical characteristics of BPs

BPs	Abbreviation	Formulae	Molar mass (g mol^{-1})	Water solubility (mg/L)	Melting point (°C)	Log $K_{o/w}$	pKa
Bisphenol A	BPA	$C_{15}H_{16}O_2$	228.29	120	158	2.2–3.8	9.78–10.39
Bisphenol S	BPS	$C_{12}H_{10}O_4S$	250.29	3,518	245–250	1.65	7.42–8.03
Bisphenol F	BPF	$C_{13}H_{12}O_2$	200.237	408.1	162.5	3.46	9.84–10.45
Bisphenol E	BPE	$C_{14}H_{14}O_2$	214.26	265	125	3.74	9.81–10.42
Bisphenol AF	BPAF	$C_{15}H_{10}F_6O_2$	336.233	0.8	162	4.47	9.13–9.74

advantages for pollution prevention and remediation. It is eco-friendly because it incorporates a pure reagent, the electron, and requires minimal or no chemical addition. Similarly, electrochemical oxidation is distinguished by its simple equipment, convenient operation, and short retention time. Other benefits include robustness, adaptability, and automation capabilities. The main disadvantage of this procedure is its high operating cost due to increased energy consumption (Anglada *et al.* 2009). In the membrane separation process, various commercial membranes from multiple manufacturers are available, many applications and module configurations are available, and a small amount of space is required. Even at high concentrations, it is simple, quick, and efficient, producing high-quality treated effluent with no chemicals. Although little solid waste is generated, the investment costs can be prohibitively high for small and medium-sized businesses (Morin-Crini *et al.* 2019). Though, we consider a cost-effective, sustainable approach, the adsorption and photocatalytic degradation show the synergistic benefits on material sizeable interfacial area, negative zeta potential, and simplified charge separation, which are primarily responsible for the integrated system's substantial improvement (Liu *et al.* 2017).

2.1. Adsorption

Adsorption is a surface phenomenon used in primary treatment methods to address hazardous pollutants at low concentrations measured in parts per million (ppm) (Figure 1). It has been identified as a suitable technology for water and wastewater treatment due to its high efficiency in diluted solutions, operating elasticity, versatile strategy, comfort handling, and cost-effectiveness. Compared to different treatment approaches, the adsorption method has shown the most favourable results for removing dissolved inorganic and organic pollutants from the aqueous phase (Miriyam *et al.* 2022). However, several variables affect both the financial and technical aspects of adsorption operation, such as adsorbent material properties, target adsorbate, accessibility, moisture, operating parameters, adsorbent recovery, and disposal methods (Barquilha & Braga 2021). Adsorption happens when an absorbable solute solution contacts a solid with a highly porous surface structure. It is based on developing an adsorbed phase that differs from the bulk fluid phase in composition (Rathi & Kumar 2021). Organic contaminants seem very resistant to several water-based treatment processes because of their hydrophobic nature and low molecular mass. In adsorption, unstable molecules are attracted to adsorbent material surfaces by diffusing from the group of the solution to the functional sites of adsorbent materials (Zango *et al.* 2020). One of the desirable properties of adsorbent materials is the physical characteristics of the adsorbent condition, typically in the form of powder, cake, or beads. Adsorption processes are influenced by factors such as solubility, molecular size, molecular weight, and pKa, in addition to the physical properties of the adsorbents (Moreno-Castilla 2004). The adsorbate molecules that have been adsorbed must be desorbed to renew and reuse the adsorbent for another cycle. During the desorption process, the solid adsorbent has the potential to be one of the most impactful ways to treat and remove organic pollutants from wastewater (Rajabi *et al.* 2018). The reversal of adsorption occurs when molecules that have adhered to the adsorbent are released back into the solution. Regenerating and reusing adsorbents in adsorption procedures significantly reduces

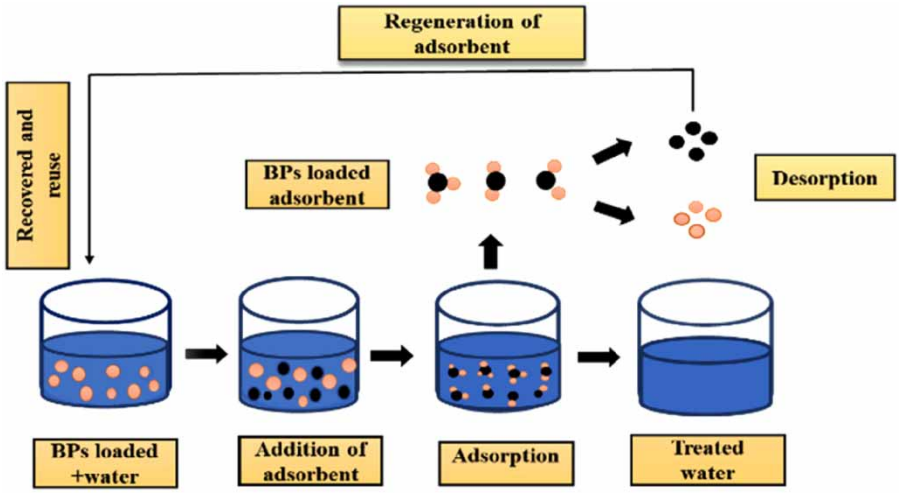

Figure 1 | Adsorption and desorption of BPs.

industrial wastewater treatment costs (Vakili *et al.* 2017). In desorption, acid and alkali solutions are commonly used to restore waste material (Duan *et al.* 2020). As a result, investigating the adsorption method for removing BPs from wastewater is essential (Duan *et al.* 2014).

2.1.1. Low-cost adsorbents

Cost analysis is one of the most important things to consider when choosing a water treatment system. The cost of the adsorbent determines the cost of the adsorbent used in the process. Researchers seek readily available, cost-effective adsorbents to remove EDCs and turn wastes into wealth. Organic chemicals and low-cost by-products from the agricultural, domestic, and industrial sectors have all been identified as viable wastewater treatment options. They facilitate the detoxification of pollutants from the effluent and its reduction, recovery, and subsequent utilization (De Gisi *et al.* 2016). The use of inexpensive adsorbents to treat BPs has been the topic of numerous research studies.

Dehghani *et al.* (2016) studied the effectiveness of BPA removal utilizing two different chitosan samples, a commercial chitosan sample purchased commercially, and a chitosan adsorbent made from waste seafood shell that is safe and environmentally friendly, non-toxic, and naturally occurring polymeric compound. In this investigation, the most excellent BPA adsorption removal rate was found at pH 5, with a 75-min contact period, and an adsorbent dosage of 0.06 g/L. The greatest sorption capacity was achieved at 34.48 and 27.02 mg/g for synthetic chitosan (SC) and commercial chitosan (CC). To remove BPF and BPS, Wang *et al.* (2021) utilized heteroatom (N/S) doped porous carbon-based materials manufactured from chicken feathers as a sustainable precursor. These materials were fabricated as a dual activation process to produce dual-doped heteroatoms with a 3D hierarchically porous structure (MZ-NSPC), within 30 min of equilibrium time it reached maximum sorption capacity at 308.7 mg/g for BPS and 295.8 mg/g for BPF. The adsorbent material reusability efficiency reduction after five repeats is 6.15%. Balci & Erkurt (2017) investigated Eucalyptus camaldulensis bark/magnetite composite (EBMC) as a low-cost adsorbent for BPA removal. At pH 7 and 50 °C, the combined eucalyptus camaldulensis bark and magnetite were shown to have a maximum sorption capacity of 290.6 mg/g. The Freundlich isotherm model better represented the adsorption process than the Langmuir, Dubinin-Radushkevich, Jovanovic, and Vieth-Sladek isotherm models. The adsorption capacity of the EBMC increased significantly from 57.08 to 290.6 mg/g when the adsorbent dosage was reduced from 0.7 to 0.1 g. The increase in adsorption capability with decreasing EBMC dosage is due to a concentration gradient between the concentration of BPA in the solution and on the surface of EBMC. It was also discovered that increasing the adsorbent mass from 0.1 to 0.7 g enhanced the percentage of BPA removal efficiency from 72.6 to 99.8%. This is due to the increase in the availability of surface-active sites with increasing doses of EBMC. It was also observed that 0.2 g EBMC was enough to eliminate 200 mg/L BPA with a 90% effectiveness. The activated carbon (AC) from fruit bunch waste is a superior, low-cost bio-adsorbent modifying with $ZnCl_2$ as a chemical reacting agent and assessing its ability to eliminate BPA from an aqueous solution was studied by Wirasnita *et al.* (2014). Throughout the 96 h, the optimum adsorption equilibrium was achieved after 48 h, with a percentage BPA elimination of 96.1% and an adsorption ability of 19.3 mg/g. Because of the abundance of readily available sites, the adsorption process began rapidly within 18 h, followed by slower adsorption over the initial 18–48 h. After 48 h, a peak was noticed, proving that the AC was saturated. While having significant adsorption capacity for adsorption, EFB-AC has a drawback. To reach equilibrium, the EFB-AC requires a more extended adsorption period. Lazim *et al.* (2015) examined the BPA removal from water using an agro-based low-cost adsorbent like coir pith, durian peel, and coconut shell (CP, DP, CS) treated with H_2SO_4. In comparison to DP and CS, the CP shows the highest sorption potential of 4.308 mg/g with 72% removal for 24 h, followed by 70% removal of DP with 4.178 mg/g and CS with 69% removal of 4.159 mg/g, asserting the ability of modified phyto-waste as the best option as an alternative adsorbent. Vidovix *et al.* (2021) provide a basic summary of how babassu-AC has great potential for usage in dirty water restoration. Under ideal experimental conditions with 318 K, 1 g/L adsorbent concentration, and 720 min equilibrium duration the maximum adsorptive capacity was achieved at 49.61 mg/g, therefore the empty fruit bunch is a good choice as a cost-effective bio-adsorbent for EDCs removal. Fibric peat was treated with hexadecyltrimethylammonium bromide (HTAB), and its effectiveness as a low-cost sorbent for removing BPA was examined by Zhou *et al.* (2011). At an initial concentration of 45 mg/L, the maximum sorption capacity of 31.40 mg/g was attained. Freundlich isotherm perfectly describes BPA sorption to HTAB-modified peat, while Langmuir isotherm best describes BPA sorption to untreated peat. Unlike unmodified fibric peat, the modified peat removed more BPA molecules and had a much lower desorption rate. According to research, the major mechanism is improved hydrophobic interaction and chemical modification of the peat surface, dramatically boosting sorption capacity towards organic compounds

dissolved in water. According to the observations, the feasible usage of low-cost adsorbents has yielded positive results in removing EDCs (Hacıosmanoğlu *et al.* 2019).

2.1.2. Carbon and polymer-based adsorbents

Carbon materials derived from porous carbohydrates or natural polymers are popular nowadays due to their superior properties, such as extremely high surface area, promising chemical stability, and high electrical conductivity (Wang *et al.* 2020). Adsorbent materials such as graphene oxide (Xu *et al.* 2013), carbon nanotubes (Naeemullah & Tuzen 2019), porous carbon materials (Bhadra *et al.* 2018), and AC (Sotelo *et al.* 2013) have long sparked the curiosity of researchers due to their chemical stability, large pore size distribution, and mass production feasibility (Tagliavini *et al.* 2017). In recent decades adsorbents made of natural polymers (Crini 2005), carbon materials, mainly ACs and their composite have acquired significant recognition as ubiquitous adsorbents due to their abundant resources like favourable physical and chemical properties, strong sorption capacity, and surface reactivity by the presence of various functional groups. Eventually, some techniques have been considered to produce more practical and cost-effective results. Carbons derived from various sources, including tea leaves (Ahsan *et al.* 2018a, 2018b), walnut shells (Dovi *et al.* 2021), coffee waste (Naganathan *et al.* 2021), rice husks (Balarak *et al.* 2019), and peanut shells (Chu *et al.* 2017), have all been used to treat wastewater and remove EDCs, according to investigation.

(Soni & Padmaja 2014) found that BPA adheres to palm shell activated carbon (PSAC) through p-p interactions and hydrogen bonding with an adsorption capacity of 62.5 mg/g. After 8 h, the BPA adsorption equilibrium was attained. The ability of BPA to connect to PAC was significantly influenced by basic pH, this is likely because both BPA and PAC zero-point charge (ZPC) deprotonated at this pH. Similarly, it was shown that the ability to absorb BPA was not greatly affected by adding 0.5 M NaCl. Film diffusion is the stage that determines the rate in the intraparticle and film diffusion process, and both of these have been discovered to regulate adsorption kinetics. According to observations of Andreia (Alves *et al.* 2019), chemically treated coffee grounds AC has a specific surface area (1,039 m^2/g) higher than physical AC making it more effective for adsorption. The Langmuir isotherm and pseudo-second-order model were used to analyze the BPA adsorption data, showing that chemical AC had a 123.22 mg/g highest sorption potential. The outcomes demonstrated that chemically treated might be a viable sorption material waste for water treatment. Guo *et al.* (2011) produced magnetic composites made of chitosan, fly ash cenospheres, and iron oxide (CTS/-Fe_2O_3/FACs) to remove BPA quickly. The CTS/-Fe_2O_3/FACs that were produced had a perfectly spherical shape, thermal stability, and saturation magnetization. The monolayer adsorption capacities for BPA and 31.92 mg/g, at 298 K, respectively. The Langmuir isotherm model had the best fit with the equilibrium compared to other models. For kinetic, the pseudo-second-order equation provided a good description for CTS/-Fe_2O_3/FACs adsorbents. With rising concentration and temperature, intraparticle diffusion (ki) and film diffusion increased, whereas pore diffusion decreased. According to the Scanning electron microscopic (SEM) images, the imprinted layer efficiently covered a considerable section of the KLT/Fe_3O_4. The adsorption capacity decreased considerably from pH 7.0 to 10.0 due to its pKa value of 10.23, making it easier to dissociate under alkaline conditions. At increasing pH, the electrostatic repulsive interactions between BPA and adsorbents get stronger and finally outnumber the binding affinity. Using magnetite and the adsorption technique, Orimolade *et al.* (2018) investigated the effectiveness of eliminating BPA from water. At a pH 6, the optimum adsorption parameter was 0.2 g dosage, at 50 ppm of BPA, with 60 min of contact time. Iron nanoparticle-doped magnetic ordered mesoporous carbon (Fe/OMC) was created by carbothermal reduction and impregnation techniques and employed for the highly efficient adsorption and degradation of BPA (Tang *et al.* 2016).

Batch studies were carried out to investigate the decontamination performance. The findings revealed that with an initial BPA concentration of 200 mg/L, the adsorption capacity had achieved 311 mg/g. The kinetic investigation indicated that it concurred well with the pseudo-second-order model. Ahsan *et al.* (2018a, 2018b) described a simplified method to produce sulphonic acid that contacts with a carbonaceous adsorbent derived from tea leaves (TW-SO_3H). At 25 °C, BPA has been removed by TW-SO_3H with a sorption capacity of 236.80 mg/g. Park & Jhung (2021) investigated the adsorptive purification of BPS-polluted water using metal-organic frameworks (MIL-101-NH_2). At pH 7, it had a maximum sorption at 513 mg/g. Additionally, the MOF is reusable, with just a little performance following ethanol washing. Second, good adsorption is mostly explained by H-bonding between the BPS and the applied MOF. Fang *et al.* (2018) showed that a magnesium ascorbyl phosphate non-shell graphene-based monolith (MAP-GBM) is a viable adsorbent for the efficient and cost-effective removal of low-concentration EDCs. MAP-GBM has a maximum sorption capacity of 324 mg/g, with 100% removal of BPS from solution at low concentrations of 50 mg/L. Soaking the material in methanol for 24 h may be readily replenished, and after five

regenerations, the adsorption efficacy stays as high as 88%. Multi-walled carbon nanotubes coated with $CoFe_2O_4$ nanoparticles improved the sorption and characterization of their abilities, according to an investigation done by Al-Musawi *et al.* (2022). The highest sorption capacity of MWCNTs/$CoFe_2O_4$ fits with the Langmuir model for BPA adsorption which was 416.6 mg/g, significantly higher than earlier reports using adsorbents for the same purpose. Bhatia & Datta (2019) studied the adsorption performance of amine-modified multiwall carbon nanotubes in batch studies and discovered that the equilibrium duration for batch adsorption tests was 45 min and the optimal adsorbent dosage was 1.6 g/L.

For the column study, increased bed height and lowered flow rate promote BPA adsorption. However, BPA concentrations are more significant at 40 mg/L, and temperatures greater than 323 K reflect unfavourable adsorption conditions. Although it has multiple regeneration properties in batch mode, the adsorbent is ineffective for BPA removal. The pseudo-second-order kinetic model best fitted the adsorption data, whereas the equilibrium data best fit the Toth and Sips isotherm models for the column test. Goyal *et al.* (2018) used hydrothermal treatment and surfactant HDTMA-Br modification to create a nano-zeolite secondary mobil-5 (NZSM-5). The functionalized nano-zeolite FNZSM-5 was utilized for rapid removal of BPS from the aqueous phase. The FNZSM-5 removed BPS higher than NZSM-1 with an efficiency of (95–36%). The electrostatic effect of solution pH from 2 to 4 significantly impacted BPS adsorption onto the produced adsorbent with optimum removal of 95%. The best match for the kinetic data was a pseudo-second-order kinetic model that represents the occurrence of chemical adsorption in the sorption system. The thermodynamic properties revealed that BPS adsorption was more beneficial at low temperatures. Zhang *et al.* (2013) investigated the removal and recovery of BPF using multiwall carbon nanotubes and discovered that the removal percentages of BPF could reach up to 96.2% in 4 min at pH 4–10. The kinetics of BPF adsorption was rapid, with the equilibrium reached in 4 min using the pseudo-second-order model and measured rate constants (k) at varied temperatures. Multi-walled carbon nanotubes modified with iron oxide and manganese dioxide (MWCNTs-$Fe_3O_4MnO_2$) were employed as an adsorbent to eliminate BPA (Guo *et al.* 2020). The maximum adsorption capacity and contact time to achieve equilibrium of initial concentrations were determined to be 132.9 mg/g and 150 min, respectively. According to the scanning electron microscopic (SEM) images, the imprinted layer efficiently covered a considerable section of the KLT/Fe_3O_4. The adsorption capacity decreased considerably from pH 7.0 to 10.0 due to its pKa value of 10.23, making it easier to dissociate under alkaline conditions. At increasing pH, the electrostatic repulsive interactions between BPA and adsorbents get stronger and finally outnumber the binding affinity. Consequently, when the pH increased above 7.0, the adsorption capacity of BPA for both MMIPs and MNIPs dropped considerably compared to the alterations observed under acidic conditions. Joseph *et al.* (2011) investigated the sorption behaviour of BPA from landfill leachate onto single-walled carbon nanotubes (SWCNTs). Solutions of artificial seawater, brackish water, and a combination of these two fluids were generated by previously published composition data. The higher removal efficiency of BPA is 75–80%, owing to a higher log K_{ow} value. Single-walled carbon nanotubes were successfully used to adsorb BPA from aqueous environments before and after the treatment of SWNTs and tSWNTs (Zaib *et al.* 2012). After a 72-h contact time at 315 K, 14.3 mg/g of BPA was adsorbed on SWNTs and 5.1 mg/g on tSWNTs. Naeemullah & Tuzen (2019) evaluated the efficiency of carbon nanotubes functionalized with tetra ethylene pentamine for surface adsorption. The monolayer adsorption capacity of the functionalized tetra ethylene pentamine immobilized on the surface of multi-wall carbon nanotubes for BPA was found to be 45.5 mg/g at pH 6.5 at 30 °C with a contact time of 40 min. As a result, carbon and polymer-based absorbents can give high adsorption capacity and may eliminate EDCs within a short contact time.

2.1.3. Biosorbents

Biosorption has long been considered an excellent approach for removing a broad spectrum of organic contaminants. The word 'biosorption' refers to any system in which a solid surface of a biological matrix interacts with a sorbate, decreasing the sorbate concentration in the solution (Fomina & Gadd 2014). The adsorption of BPA from aqueous solutions using biosorbent materials such as peat, rice husk, bagasse, and sawdust was examined by Zhou *et al.* (2011) in contrast to the other materials taken into consideration. The surface of the peat developed a selectivity for BPA after being treated with alkyl ammonium. Modified peat had a slightly higher sorption capacity of 1.71 mg/g than AC of 1.67 mg/g under specific conditions with a BPA concentration of 2 mg/L. Ahsan *et al.* (2018a, 2018b) demonstrates synthesizing a simple sulphonation method to produce sulphonated coffee waste with superior biosorption potential for a wide range of emerging pollutants. This biosorbent was used in wastewater to remove endocrine disruptors such as BPA and sulphamethoxazole (SMX) medications. The biosorption capacities of CW-SO_3H for BPA and SMX removal were 271 and 256 mg/g, respectively. BPA adsorption from an aqueous solution on inactivated lichen biomass (*Pseudoevernia furfuracea*) was investigated by Şenol

et al. (2020). The maximum removal occurs at pH 5 for 3 h, then an adsorbent dosage with an initial concentration at 40 mg/L,9 mg/g, and 150 rpm. Sorption capacity reached 82% after eight cycles, with a 5% reduction in the regaining rate. Li *et al.* (2017) examined the effect of ash concentration on BPA sorption utilizing various agricultural waste as adsorbents like silkworm dung, corncob eucalyptus globulus, and pomelo peel, observed that the acid treatment substantially enhanced BPA adsorption capacity. Biosorbent material has effectively removed EDC contaminants from the aqueous environment.

2.1.4. AC-based adsorbents

AC is a mesoporous carbon-containing material that has become a commonly used sorbent material because of its large surface area, inexpensive, and excellent charge-holding capabilities, as well as the capacity to produce multiple functional groups which could be responsible for the effective removal of a wide range of contaminants from water-soluble or gaseous media (Sabzehmeidani *et al.* 2021). AC is available in granular, powdered, and fibrous forms, all of which are widely used in water remediation methods (Jjagwe *et al.* 2021). Because of its excellent adsorption capacity, AC has been successfully used to remove pollutants such as colours, CO_2, and phenolic and organic chemicals (Kalderis *et al.* 2008). According to Tagliavini *et al.* (2017), AC is one of the most effective adsorbents. Still, it has various disadvantages, such as being flammable and difficult to regenerate, limiting its usage in wastewater treatment.

Sudhakar *et al.* (2016) examined the use of activated rice husk (RHA) as an adsorbent for BPA recovery from aqueous solution and contrasted its performance to that of granular activated carbon (GAC). RHA had the best values at a concentration of 100 mg/L and the dosage at 30 g/L with a contact time of 3 h for RHA. In contrast, the optimum parameters of GAC were found to be 20 g/L of dosage with a contact time of 2 h. The Freundlich and Temkin models pseudo-second-order model, and the pseudo-second-order model provided the best fits for the isotherm data and the adsorption kinetic data, respectively. It was discovered that the BPA adsorption onto GAC and RHA was endothermic. AC combined with constructed wetlands (CWs) was used as an adsorbent for BPA, BPS, and BPF pollutants. The findings indicate that the fundamental mechanism of the AC-CW's efficient and stable removal of EDCs was a two-step process in which EDCs were initially adsorbed onto the AC and subsequently eliminated by the sizeable bacterial population on the AC.AC-CW totally and sustainably eradicated all EDCs 98–100%. The addition of AC as a component of the CW medium could increase EDC removal (Wirasnita *et al.* 2018). To eliminate BPA from aqueous solutions, iron oxide goethite particles with activated carbon (GPAC) have been suggested by Koduru *et al.* (2016). At the initial concentration of 10 ppm at pH 7, BPA was promptly removed at 100 min; equilibrium was slowly restored after 200 min of shaking. XRD patterns of pure iron oxide and AC/iron oxide goethite composites revealed the crystalline nature of goethite. The capacity of AC to remove BPS by adsorption from deionized water has been widely demonstrated by Zhao *et al.* (2022). This ability is strongly inclined through environmental factors such as temperature and pH. The research reveals that BPs adsorption is more significant in deionized water than in tap water, making it harder for AC aquatic filters to recover BPS from tap water. After pH 6, the removal rate and adsorption capacity progressively declined. The contact time was around 50 min, with the amount of adsorption capacity of 83.19 mg/g. Chemically treated AC was more successful than physically treated AC in BPA removal due to its greater surface area. The pseudo-second-order model for kinetics computed the BPA adsorption data, and the Langmuir model for isothermal study, revealing a maximum chemical AC adsorption capacity occurred at 123.22 mg/g. Rice straw-AC can potentially remove BPA from the environmental matrices investigated (Chang *et al.* 2012). The adsorbent was prepared using potassium hydroxide KOH to convert waste biomass into AC. The AC absorbs BPA quickly due to its maximum surface area and adsorptive capacity of 181.19 mg/g. Reaching equilibrium at 90 min at 30 °C. BPA sorption capability in babassu-AC was investigated by Ahamad *et al.* (2019) developed a highly permeable N/S-modified magnetic carbon nanocomposite (N/S-MCA) from sugarcane bagasse-based cellulose and utilized it for BPA removal. According to the findings, the mechanism of synergistic adsorption of BPA using N/S-doped magnetic carbon aerogel would be an essential guideline in developing a carbon-based adsorbent for the high-efficiency adsorption of environmental pollutants.

2.1.5. Surfactant-modified adsorbents

Surface active agents are surfactant compounds that can modify the surface energy between the substances (Tamjidi *et al.* 2021). This property is related to its dipolar molecular structure, which contains amphiphilic or amphipathic molecules that contain polar (the hydrophilic portion that is soluble in a particular fluid, such as water) and nonpolar (the hydrophobic element that is insoluble in water). The term 'amphi' is derived from the Greek word which means 'both' (Belhaj *et al.* 2020). Adsorbents with a modified surfactant base were a great option. As a result, it has been demonstrated that using surfactants as

a modifier for removing organic contaminants significantly improves the ability of diverse materials to adsorb pollutants (Lawal *et al.* 2019).

The adsorption of BPA onto natural bentonite modified hexadecyl trimethylammonium chloride (HDTMA) was investigated by (Genc *et al.* 2019). Due to a neutral molecular form of BPA and the hydrophobic surface produced by the loaded surfactant molecules, BPA removal was accelerated under acidic pH conditions. When the ionic strength was increased, the BPA adsorption on modified bentonite was improved, and the adsorption capacity was attained at 15.63 mg/g. Tang *et al.* (2017) investigated a one-step technique that dispersed AC-AB, CTAB and synthesized AC-AB-CTAB prepared for the BPAF removal from wastewater. The one-step method outperforms the synthesized adsorbents with a maximum reduction of BPAF of about 284.6 mg/g. Kinetic investigations and adsorption isotherms revealed that the one-step adsorption of BPAF on AC-AB could be represented by a pseudo-second-order model and a Dubinin-Ashtakhov (D-A) isotherm, respectively. Bamboo fibre powders were recognized by Hartono *et al.* (2015) as a promising low-cost sorbent with superior adsorption properties for eliminating hazardous organic chemicals in aqueous systems. Treating the bamboo powders with alkali and surfactants seemed to be enhancing the BPA sorption performance with 39% removal obtained for bamboo treatment with the cationic surfactant with an adsorbent dosage of 4 g/L. Zheng *et al.* (2013) investigated Organo Arizona SAz-2 Ca-montmorillonite generated by direct ion exchange with different surfactant (DDTMA and HDTMA) loadings to remove BPA. The monolayer pattern with minimal surfactant loading, hydrophobic phase (0.5 CEC), and positively charged surface produced by the loaded surfactant molecules enhances the BPA adsorption. The values for DDTMA slightly increased from 1.94 to 2.03 nm as the CEC from 1.0 to 2.0, showing that the arrangement of DDTMA molecules in the interlayer space changes from monolayer to bilayer and that longer chain surfactant intercalated in organoclays has a better capacity for BPA adsorption even in alkaline conditions. Furthermore, the molecular conformation of the intercalated surfactant is significantly influenced by the surfactant chain length and surfactant loading. A Langmuir isotherm revealed that the highest sorption capacity for organo clays on removing BPA was 151.52 mg/g. Surfactant cetylpyridinium bromide (CPB) modified natural zeolites (SMNZs) were prepared by Li *et al.* (2014). BPA was effectively removed from the aqueous solution using monolayer and bilayer SMNZs. The monolayer SMNZs for BPA adsorption gained somewhat when pH climbed from 4 to 9 but reduced dramatically as pH increased from 9 to 11. The bilayer SMNZs for BPA adsorption were achieved between pH 9 and 10 and declined when it was reduced between 9 and 4 or increased between 10 and 11. The hydrophobic interaction and hydrogen bonding are the mechanisms for BPA adsorption onto the monolayer SMNZ at pH 4–11. Organic partitioning and hydrogen bonding are two pathways for BPA adsorption on the bilayer SMNZ at pH 4–8. At pH 8–11, electrostatic attraction, hydrogen bonding, and organic partitioning are the methods through which BPA adheres to the bilayer SMNZ. Kuang *et al.* (2019) studied to build a novel graphene oxide (GO)-based adsorbent by loading the cationic surfactant HDTMA to adsorb BPA from aqueous solution simultaneously. BPA adsorption capacities were 141.0 mg/g for the synthesized adsorbents. BPA adsorption procedures were fast, with 100% removal achieved in 2 h, respectively. Raising the pH favoured the adsorption of the BPA adsorption. The results show that by customizing the surface coverage of HDTMA on GO, adsorption of the target species may be accomplished. The summary and overview of adsorbents to be used for the adsorption of BPs are given in Table 2.

The adsorbent and BPs properties are among the most significant causes of sorption inhibition at high pH, while other variables can also impact (Miriyam *et al.* 2022). Other important parameters involved in BPs elimination are initial concentration, contact period, dosage, pH, and the temperature that affect BPs compounds to remove from an aqueous solution. Adsorption performance can be increased by extending contact duration due to abundant vacant active sites on the adsorbent surface. The availability of BPA to the active sites on the adsorbent surface would be constrained with increased contact duration, resulting in a decrease in adsorption effectiveness (Balarak *et al.* 2019). When the concentration of BPA was low, the number of adsorption sites increased in parallel with a rise in adsorbent dosage. If the concentration were too high, the adsorbent would quickly attain saturation. As a result, contaminant retention would be terminated (Martín-Lara *et al.* 2020). The weakening of the hydrogen bonding interaction caused a reduced adsorption capacity for pH. This is due to its particles forming bisphenolate anions and releasing protons in an alkaline solution. Hydrophobicity, hydrogen bond, electrostatic and π–π interactions were the main BPs sorption mechanisms onto an adsorbent (Hamadeen & Elkhatib 2022). Due to the protonated effect of functional surface molecules like amino, carboxyl, thiol, and others, the AC surface gets wholly charged. This may increase the normally hydrophobic interactions between BPs and sorbent material by adding electrostatic attractions. The neutral charge of the adsorbent and adsorbate inhibits the formation of any further sorbed mechanisms other than hydrophobic interactions. The creation of aqua-complexes, which hinder adsorption, is brought on by an increase in

Table 2 | Adsorption of BPs

Pollutants	Adsorbents	Initial concentration (mg/L)	Dosage (g/L)	Contact time (min)	pH	Adsorption capacity (mg/g)	Temperature (°C)	Cost per unit price(kg)	References
BPA	CC, SC	0.1	0.06	75	5	27.02,34.48	30		Dehghani *et al.* (2016)
BPA	Eucalyptus bark/magnetite composite	50	0.1	50	7	290.6	20		Balci & Erkurt (2017)
BPA	Activated palm shell	50	0.03	60	<7	62.5	30		Soni & Padmaja (2014)
BPA	Bentonite by hexadecyl trimethylammonium chloride (HDTMA)	100	0.025	40	<9	16	30		Genc *et al.* (2019)
BPF, BPS	N/S dual-doped porous carbon (MZ-NSPC)	110	0.1	120	<9	295.8, 308.7	35–45		Wang *et al.* (2021)
BPAF	AC-Alginate beads with etyltrimethylammonium ammonium bromide	100	0.05	1,440	–	2.233	15–35		Tang *et al.* (2017)
BPA	Iron nanoparticle-doped magnetic ordered mesoporous carbon	200	0.1	360	9	311	30		Tang *et al.* (2016)
BPA	Chitosan/-Fe2O3/fly-ash-cenospheres	–	–	60	7	31.92	25 ± 0.1		Guo *et al.* (2011)
BPF	Multi-walled carbon nanotubes	20	0.045	4	–	83	35		Zhang *et al.* (2013)

hydroxyl ions at basic pH. Temperature is another important component that influences adsorption capability. Endothermic process refers to a process where adsorption increases as temperature rises. Increased temperature improves the mobility of organic pollutants, resulting in quicker adsorption owing to easier access of adsorbate to adsorbent. Exothermic processes are those in which adsorption capacity reduces with increasing temperature, greater the temperature, lower the adsorptive forces between adsorbate and adsorbent has been occurring (Saxena *et al.* 2020).

2.1.6. Cost analysis

Table 2 lists the readily accessible adsorbent raw materials (such as agricultural wastes, clays, polymer materials, chitosan, nanoparticles, graphene, and carbon nanotubes) used in adsorption processes.

(a) **Agricultural waste materials**: Agro-waste materials are dumped in the soil without any use. Still, they but they contain several essential elements such as lipids, lignin, cellulose, hemicellulose, hydrocarbons, extracts, proteins, starch, simple carbohydrates, and water, as well as a variety of functional groups that present in the binding process and can sequester pollutant. Agricultural wastes are inexpensive in cost, easily accessible, and have plenty of assets and distinctive chemical structures, so they frequently get used to examining the removal of contaminants from water-based solutions (Lazim *et al.* 2015). Using chemical activation with the agricultural waste is found to be more expensive than the raw agro-waste adsorbents, since the adsorption capacity is more in chemically activated than physical method.

(b) **Clays:** Clay minerals have historically been prominent in their function as an adsorbent for hazardous chemical disposal and storage to protect as an adsorbent for hazardous chemical disposal and storage for the protection of the environment. They are a naturally occurring substance with particles ranging from 2 m down, resulting in substantial surface areas suited for high-efficiency pollution removal. Compared with AC, organic/inorganic, and composite materials, clays and modified clay-based adsorbents are the most effective clarifying agents and low cost for organic contaminants removal (Mundkur *et al.* 2022).

(c) **AC:** AC is a broad term for a variety of carbonized materials with a high degree of porosity and surface area. The materials that are calcined at a particular temperature in a muffle furnace are known to be an AC. Commercially available AC is found to be more expensive than synthesized carbon. Among all the natural adsorbents, AC has been found to be the most effective for organic contaminant removal; however, its use is restricted due to its high regeneration cost (Heidarinejad *et al.* 2020).

(d) **Chitosan:** Chitosan has a high affinity for hydroxyl and amino groups. Because of its inexpensive cost and high adsorption potential, it is employed as an adsorbent for contaminant removal. Chitosan has also been combined with other substances, including as graphene and zeolite, to create composite materials that have better adsorption capabilities. Commercially available chitosan is more expensive than the synthesized chitosan due to its pretreatment processes (Zhang *et al.* 2021).

(e) **Nanoparticles:** Nanoparticles exhibit distinct chemical, physical, visible, electrical, magnetic, and biological properties because of their extraordinarily high specific surface area and minimized surface defects (Chen *et al.* 2017b). Plant extract-derived nanoparticles have different surface morphologies than routinely manufactured nanoparticles, contributing to the adsorption process.

3. PHOTOCATALYSIS

The possibility of utilizing solar energy seems quite attractive (Ferdous *et al.* 2016) (Figure 2). The catalytic activities initiated by light energy are known as photocatalytic activity. Because of its high mineralization efficiency, low toxigenicity, and ideal end products of carbon dioxide, water, and inorganic mineral ions, this is considered among the most promising approaches (Sharma & Vaish 2021). An advanced oxidation process (AOP) called photocatalysis is used to purify aqueous systems, and light degrades hazardous chemicals. AOP may successfully oxidize numerous organic contaminants found in aqueous systems. Though diverse reaction systems are active, all AOPs have the same essential feature forming radicals (•OH) through a multi-step process. Because of their solid oxidative capacity reduction potential, HO• radicals exhibit minimal attack selectivity and may oxidize a wide range of organic contaminants (Zhai *et al.* 2022). The significance of photocatalysis implies that a photocatalyst offers both an oxidation and a reduction simultaneously. Heterogeneous catalysis has effectively decomposed various hazardous compounds (Kumar 2017). When a semiconductor absorbs photons with an energy equal to or greater than its band gap, heterogeneous photocatalysis typically begins. The electrons are then excited from the semiconductor's valence band (VB, the highest energy band occupied by electrons) to the conduction band (CB, the lowest energy band without electrons at the ground state), generating electron (e^-) hole (h^+) pairs. As electrons and holes are transported to the semiconductor's surface, electrons react with acceptors to form reduction products, whereas holes interact with donor species to produce oxidation products; if holes and electrons are not depleted rapidly, they may recombine, resulting in energy loss.

The following is an explanation of the general mechanism of photocatalytic degradation of organic compounds:

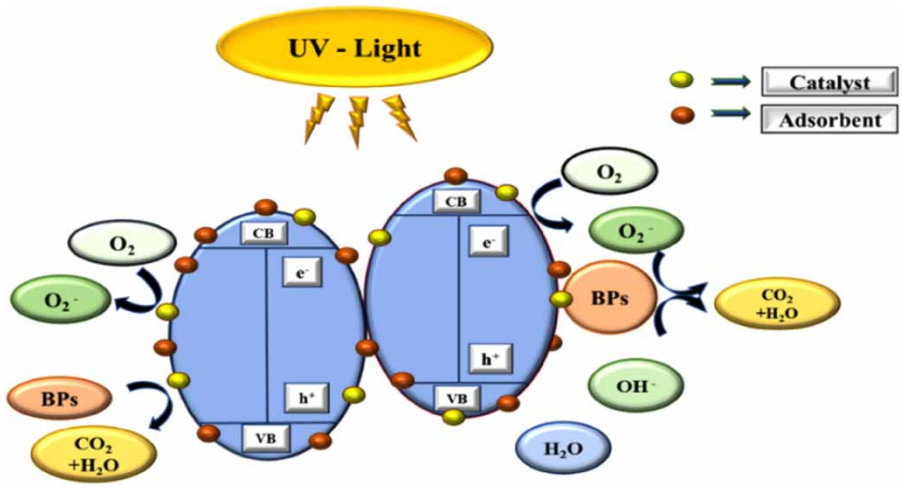

Figure 2 | Synergetic mechanism of adsorption and photocatalytic degradation of BPs.

In Equation (1), the electrons (e) are stimulated from the valence band (VB) to the conduction band (CB), and holes (h^+) are produced in the VB when the catalyst is subjected to photons with energies equal to or higher than the photocatalyst band gap energy:

$$PC + hv \rightarrow e^-_{CB} + h^+_{VB} \quad (1)$$

where hv denotes the force needed to move electrons from the conduction band to the valence band. Because of this, in Equation (2) superoxide radicals (O_2) produced by irradiation may be quickly attracted to O_2 dissolved in solution or absorbed on the photocatalyst surface:

$$eCB^- + O_2 \rightarrow O_2^{\cdot -} \quad (2)$$

As a result, when O_2 reacts with H_2O, it produces hydroperoxyl radical (HO_2) and hydroxyl radical (OH), both of which are potent oxidizing agents that destroy the organic molecule in Equation (3):

$$O_2^{\cdot -} + H_2O \rightarrow HO_2^{\cdot} + OH \quad (3)$$

At the same time, in Equations (4) and (5), surface hydroxyl groups or H_2O on the photocatalyst surface may trap photo-induced holes, resulting in hydroxyl (OH):

$$h^+_{VB} + OH^- \rightarrow \cdot OH_{ad} \quad (4)$$

$$h^+_{VB} + H_2O \rightarrow \cdot OH + H^+ \quad (5)$$

Eventually, in Equation (6) the molecules will be oxidized to produce water and carbon dioxide as follows:

$$OH + organic\ molecules + O_2 \rightarrow products(CO_2\ and\ H_2O) \quad (6)$$

Meanwhile, in Equation (7) recombination of positive hole and electron could take place, which could reduce the photocatalytic activity of the prepared nanocatalyst (Gnanaprakasam *et al.* 2015):

$$eCB^- + h^+_{VB} \rightarrow PC \quad (7)$$

The semiconductor typically absorbs photons with energy equal to or more than its band gap to begin heterogeneous photocatalysis. The formation of electron (e^-) hole (h^+) pairs occurs when electrons are stimulated from the semiconductor's valence band (VB, the highest energy band filled by electrons, to the conduction band CB, the lowest energy band devoid of electrons at the ground state). When electrons and holes are transported to the semiconductor surface, they react with acceptors to form reduction products and with donor species to produce oxidation products. But the holes and electrons could recombine and lose energy if not rapidly released (Yuan *et al.* 2021). Photocatalysis is low-cost, non-toxic, and easy to fabricate to degrade organic pollutants like EDCs. Throughout the last several decades, various photocatalysts have been created to address the difficulties of water pollution, particularly photocatalysis on semiconductor catalysts such as TiO_2 (Katančić *et al.* 2020), CuS_2 (Bahadoran *et al.* 2021), ZnO (Javid & Malakootian 2017) and MoS_2 (Kumar & Bansal 2013) has shown effectiveness in degrading a variety of organic contaminants into biodegradable or less harmful organic compounds. Doping of TiO_2 with precious metal (Pt), metal oxides such as ZnO, Fe_2O_3, and inorganic components such as N for extended visible light activities has been successfully conducted by Mühlberg (2020). Unfortunately, the poor solar energy conversion efficiency, simple aggregation, and difficult post-separation of these inorganic catalysts prevent their widespread use (Wang *et al.* 2016). RongChang *et al.* (2009) summarized BPA removal by photocatalytic degradation using TiO_2 as a catalyst along with the experimental circumstances that explain how BPA molecules and by-products can bind to the surface of the TiO_2 for their subsequent degradation, which represents the first stage of the process and in the second stage all adsorbed substrates will be broken down. The following presumptions apply to TiO_2 catalyst for BPA photocatalytic degradation on kinetic model:

(1) In Equation (8), the hydroxyl groups that are absorbed by the surface of the TiO_2 particles destroy organic molecules and associated intermediates, and the interaction with hydroxyl molecules is the rate-limiting phase in photocatalytic degradation.
(2) The formation of •OH radicals is shown in Equation (9) should be primarily derived from the adsorbed H_2O molecule as the reaction of H_2O/OH with photo-induced gap h^+ to generate hydroxyl reversibly.
(3) In the process involving h^+, H_2O, and OH, the Equation (10) shows the rate of hydroxyl production is far faster than the rate of h^+/e^- combination, and the concentration of H_2O/OH available to combine with h^+ is much higher than that of H^+.
(4) In Equation (11) the concentration of hydroxyl radicals remains constant at a steady state (Bodenstein steady-state assumption).

The elementary reaction equations for the above-mentioned photocatalytic reaction processes are as follows:

$$TiO_2^+ + hv^- \rightarrow TiO_2(e^- CB + h_{VB}^+) \tag{8}$$

$$h_{VB}^+ + OH^- \rightarrow \cdot OH \tag{9}$$

$$h_{VB}^+ + H_2O \rightarrow \cdot OH + H^+ \tag{10}$$

$$\bullet OH + BPA \rightarrow\rightarrow Oxidative\ intermediates \rightarrow\rightarrow CO_2 + H_2O \tag{11}$$

The photodecomposition reaction rate constant (k) of BPA over TiO_2 catalyst was calculated using Equation (12):

$$r = \left[\frac{k_r K_e C}{(1 + K_e C)}\right] \tag{12}$$

where k_r and K_e are the reaction constant and adsorption constant of equilibrium. The linearized rate form is expressed Equation (13):

$$\frac{1}{r_0} = \frac{(1/k_r K_e)(1/C_0) + 1}{k_r} \tag{13}$$

where C_0 is the initial BPA concentration and r_0 is the initial degradation rate. The intercept of the plot of $1/r_0$ and $1/C_0$ denotes kinetic coefficient that varies directly with the rate of degradation. The K and k values are 6 mmol/L and 0.303 mmol/L/h, respectively.

TiO_2 is a highly effective photocatalyst due to its photocatalytic activity, chemical and physical durability, affordability, and convenience. TiO_2 generates photoinduced positive holes (h^+) and electrons (e^-). The surface is illuminated by UV rays 380 nm. These species can then form hydroxyl free radicals (•OH), potent oxidants contributing to the breakdown of pollutants into CO_2 and H_2O. Mei *et al.* (2020) showed photocatalytic degradation of BPS using a TiO_2/C_3N_4 composite produced hydrothermally. To achieve adsorption equilibrium, a 450 W Xe arc lamp was swirled for 3 min in the dark with 50 mL of 20 ppm of BPA solution at pH 6. The regeneration tests were performed in the following order, after the first photodegradation experiment, TiO_2/g-C_3N_4 was filtered and centrifuged. The samples were oven dried for 12 h to remove the adsorbed TiO_2/g-C_3N_4 water. The second photodegradation experiment was carried out using the dried catalyst solid. The photodegradation period was set at 60 min in the five-cycle trials. The effects of CD with TiO_2 photocatalytic degradation of BPE were studied by Wang *et al.* (2006) utilizing a 250-W metal halide lamp with 365 nm. The concentration of BPE ranges from 2.5 to 20.0 mg/L, following pseudo-first-order. Compared to systems with only TiO_2, BPE reaction rate constant is higher with CD and TiO_2. By analyzing with UV, after 40 min of irradiation, CD could enhance photodegradation efficiency by around 26% for 10 mg/L of BPE. Bechambi *et al.* (2015) Examined the hydrothermal synthesis of carbon-doped ZnO with varied molar ratios of carbon content. As a persulphate activator, amino-functionalized metal-organic frameworks degrade BPF. The C-ZnO catalysts showed photocatalytic solid activity in the degradation of BPA with the presence of hydrogen peroxide and UV light. After 24 h of UV exposure, C-ZnO achieved 100% BPA breakdown and 70% BPA mineralization under optimal conditions. The photocatalytic degradation efficiency of BPA removal using TiO_2/reduced graphene oxide nanocomposites was investigated by Luo *et al.* (2017). At pH 5, 50.42% removal efficiency was reached in 120 min using an XPA-7 photochemical reactor (XueJiang Electromechanical Factory, China) with 12 quartz tubes around a 20 W UV lamp

254 nm, 50 mL of BPA solution and 1 g/L of catalyst. Bismuth Nitrate Bi $(NO_3)_3.5H_2O$ as a Bismuth source for enhancing the photocatalytic performance by facile method at room temperature to remove BPA (Jamil & Mansor 2018). The removal efficiency of BiOBr, BiOI, and BiOI was 55, 79, and 93%, respectively, after 120 min irradiation with a 1.0 g/L dose of photocatalysts at pH 10. As a result, heterostructure is regarded as a viable way to enhance pure photocatalysts for the breakdown of organic contaminants in water. For BPE degradation, Orona-Návar *et al.* (2021) prepared rare-earth doping (Gd^{3+}) to increase the efficiency of $BiVO_4$ photocatalysis The breakdown of BPA, BPS, and BPAF in water was used to assess how different Gd^{3+} concentrations affected the process. When the photocatalyst with the greatest Gd^{3+} concentration was utilized, using a hydrothermal method, the breakdown percentages of BPs were 77.02, 44.36, and 74.11%, respectively, after 3 h of processing. Reactive species were identified using total antioxidant tests and further kinetic studies.

Sahu *et al.* (2021) synthesized exfoliated graphitic carbon nitride exfoliated (GCN, EGCN) by treating it with acid. When exposed to short-duration visible light >420 nm, EGCN exhibits substantial valance band hole transfer for the photocatalytic mineralization of BPA. Due to the production of OH^- radicals, EGCN could remove 99% of BPA. Lv *et al.* (2021) synthesized a Z-scheme heterojunction BiOI/B4C (BOBC) for BiOI activation of peroxymonosulphate. Under ideal conditions, the BOBC could remove 90.4% of bisphenol S (BPS) in 30 min. At the same time, experiments revealed that the synergistic effects show higher activity than individual peroxymonosulphate system. Wang *et al.* (2022) developed a poryphyrinic ziroconim metal-organic framework (PCN-223) to effectively remove BPF from saline water using a visible light approach. By creating ionic connections with Zr, coexisting anions increase the conductivity of electrons, enhancing light-induced electron transfer under visible light. A novel Co_3O_4-Bi_2O_3 catalyst was produced by Hu *et al.* (2018) with microwave, and its response properties were investigated using XRD and SEM. The activity of the synthesized photocatalyst was tested for its ability to degrade BPA as a peroxymonosulphate (PMS) activator. The findings show that the catalyst accelerated BPA degradation with catalytic conditions of 0.1 g/L and five molar ratios of PMS/BPA, exhibiting 100% BPA degradation within 15 min. While the pH of the solution ranged from 3 to 11, the dual-loaded catalyst system demonstrated better activity. By activating peroxymonosulphate (PMS) to create free radicals, amorphous boron (A-boron) can be employed as a metal-free catalyst for the efficient degradation of BPS, according to research by Shao *et al.* (2017). It demonstrated remarkable catalytic activity and superior stability compared to carbon-based catalysts made from metal. Zhang & Chu (2022) used physical mixing to create a dual photocatalyst of Zn-TiO_2 and Cu-TiO_2 for BPS degradation. The Zn-TiO_2 and the hydrolysis of persulphate in the system both produce superoxide radicals, which can speed up the Cu(II)/Cu(I) redox cycles and have a synergistic effect and it provided an efficient way of improving the reaction by merely combining two catalysts, as well as the mechanism underlying the synergistic benefit. Wu *et al.* (2020) developed several iron and nitrogen co-doped porous carbon catalysts (Fe-N/C) by pyrolyzing Fe-doped zeolitic imidazolate framework-8. The breakdown of BPF by activation of PMS, the doped catalytic performance, was assessed. The optimal 1.0% of Fe-N/C showed exceptional performance for PMS activation, outperforming the traditional catalyst Co_3O_4. Also, it was determined that single oxygen was the dominating reactive species, displaying specific selectivity for organic pollutants and high resilience to the pH and water matrices in the 1.0% Fe-N/C-PMS system. The photocatalytic degradation of BPs is outlined in Table 3.

4. SYNERGETIC REMOVAL OF BISPHENOL AND ITS ANALOGUES BY ADSORPTION-PHOTOCATALYSIS

The benefit of combining photocatalysis and adsorption is a feature of synergistic processes. Such benefits consist of high efficiency, inexpensive, widespread availability of adsorbates, superior recoverability, and reduced secondary pollution. The adsorption process can aid in reducing contaminant accumulation on the catalyst surface caused by wastewater, thereby improving photocatalytic degradation efficiency. Photocatalysis can eventually mineralize contaminants to H_2O and CO_2 when exposed to light at room temperature, trying to replicate the catalyst's surface for the next adsorption process. As a result, this synergistic adsorption and photocatalytic degradation will provide useful insights for developing highly efficient and sustainable wastewater clean-up materials (Xu *et al.* 2020). Photogenerated electron and hole (e^-/h^+) pairs are produced by photocatalysts when exposed to radiation (Chen *et al.* 2016b). The pairs participate in a subsequent process that generates active species such as superoxide and hydroxyl radicals (Li *et al.* 2012). Radicals that are created react with pollutants to transform them into less harmful molecules. Semiconductors with a broad bandgap, high photosensitivity, and photochemical stability, such as ZnO, TiO_2, ZnS and BiOBr, are good options for use in photocatalysis (Ahmed *et al.* 2021). Some semiconductors having less quantum efficiency due to the fast recombination of e^-/h^+ pairs. In order to overcome this constraint, numerous compounds have been doped into catalysts as electron scavenging agents (Sudhaik *et al.* 2018) like Ba, Ag,

Table 3 | Photocatalytic degradation of BPs

Pollutants	Catalyst	Initial concentration (mg/L)	Temperature (°C)	pH	Light	Efficiency, %	Contact time (min)	Refs.
BPE	Cyclodextrin (CD) on TiO_2	10	–	6	–	26	120	Wang *et al.* (2006)
BPF	PCN-233	15	Room temperature	–	500 W xenon lamp	80	60	Wang *et al.* (2022)
BPA, BPS, BPAF	Active Gd^{3+} doped $BiVO_4$	10	25	–	visible LED lamps	77, 44.36, 74.11	180	Orona-Návar *et al.* (2021)
BPS	$BiOI/B_4C$	5	25 ± 1	7	300 W xenon lamp	90.4	15	Zhang & Chu (2022)
BPA	Bismuth nitrate bi $(NO_5)_3.5H_2O$	20	–		Photochemicalreactor 1,000 W Xe lamp	99	60	Jamil & Mansor (2018)
BPA	Metal free 2D graphitic carbon nitride	2	25	7	300 W xenon lamp	60	120	Sahu *et al.* (2021)
BPA	Peroxymonosulphate with $CO_3O^{4-}Bi_2O_3$	20	25	7.34	–	45.2	30	Hu *et al.* (2018)
BPS	Peroxymonosulphate by amorphous boron	10	–	7	–	48–100	150	Shao *et al.* (2017)
BPS	Cu-TiO_2 Zn-TiO_2	0.05–0.2	–	–	UV-LED	100	18	Zhang & Chu (2022)
BPF	C catalysts doped by Fe and N	10	–	7	–	97.1	90	Wu *et al.* (2020)

non-metal dopant such as C, N, carbon dots, Mn, Cu, hydrogels, carbon nanotubes, AC, graphene-like nanomaterials, and chitosan for the catalyst support. Incorporating materials on catalysts enhances the catalyst efficiency by scavenging electrons, strengthening surface absorption of impurities, assisting as a photosensitizer, and improving visible light absorption (Brandsma *et al.* 2022). By providing more surface area, it has been discovered that surface area plays a crucial role in the degradation of organic pollutants in a synergistic method (Natarajan *et al.* 2018). Organic contaminants like EDCs were easily adsorbed onto the photocatalyst surface with a high probability, were rapidly degraded (Kanan *et al.* 2020).

Meng *et al.* (2017) demonstrated that under visible light, a zirconium-porphyrin metal-organic framework (MOF) catalyst could control photodegradation and adsorption and allow for kinetic separation. This synergistic effect increases photocatalytic efficiency and confirms that catalysis occurs within the pores of the MOF rather than in solution. Even with very high sorption uptake 487.6 mg/g, efficient photodegradation could be observed < 20 min. Zhang *et al.* (2018) developed an effective titanium dioxide 3D graphene hydrogel (TiO_2-rGH) to remove BPA from wastewater using a simple one-pot method. The TiO_2-rGH has a porous structure that promotes the attachment of extra nanoparticles with defined surface areas and active regions larger than those of the thin film electrode. Because graphene has high conductivity, the TiO_2-graphene hydrogel conducts charges quickly and solves the low conductivity problem. In 5 h, the synergistic effect of the TiO_2-rGH electrode destroyed the 20 mg/L of BPA. After 10 cycles with self-regeneration properties, removal capacity is still greater than 90%. Without filters, it is easy to accomplish quick separation and regeneration. The Fe_3O_4-biochar (Fe_3O_4-BC) heterogeneous catalyst with peroxymonosulphate (Fe_3O_4-BC/PMS) was prepared by (Cui *et al.* 2021) examined the mechanism of sorbent to eradicate BPA and it reached 100% in 90 min at pH 3.0, with PMS at 5 mM, Fe_3O_4-BC load at 2.0 g/L, and BPA at 20 mg/L. The Fe_3O_4-BC catalyst retained its high activity after five recycles with an iron loss of just 2.13 mg/L at pH 3.0, highlighting its catalyst's excellent potential for reuse and appropriateness for various applications. Zhu *et al.* (2018) used a hydrogel catalyst (P(HEA-co-HAM)-CdS) to eliminate BPA from aqueous. Under 500W visible light irradiation, the BPA breakdown rate of developed hydrogel reached 92% in 3 h. Photocatalytic oxidative radicals detecting investigations demonstrated that both holes h^+ and O_2^- play a significant part in such systems, with the degradation rates of BPA reaching 47%. Luo *et al.* (2017) produces a titanium dioxide/molybdenum disulphide-reduced graphene oxide ternary hybrid (TiO_2-MoS_2-RGO) photocatalyst for BPA removal. At a catalyst dosage of 0.5 g/L and an initial BPA concentration of 10 mg/L, the breakdown was observed at pH 5. The BPA had adsorption removal ratios of TiO_2, TiO_2-MoS_2, TiO_2-RGO, and TiO_2-1MoS_2-RGO was 0.75, 0.79, 2.30, 24.00, and 22.10%, respectively. The results indicated that TiO_2 hydrophilic nature limits its capacity to adsorb hydrophobic BPA when subjected to UV irradiation. When those catalysts are combined, it improves the effectiveness of both adsorption and degradation. Qu *et al.* (2012) investigated the behaviour of poplar leaves to eliminate EDCs by heating poplar leaves in air to 450 °C. Carbon nanotubes (CNTs) were created by heating poplar leaves in air to 723.15 k. CNTs had outer and inner diameters of roughly 77.5 and 40.1 nm, respectively, and were made up of C, O, Na, Zn, Cu, Ca, K, Cl, and S. The statistics show that without CNTs, BPA degradation was about 24.5–4.7% 180 min with solar light irradiation. The total equilibrium period of BPA adsorption/desorption onto the surface of CNTs was less than 30 min, and CNTs absorbed approximately 19.7% of BPA. Following that, the photodegradation efficiency of BPA was enhanced to 74.8 by combining CNTs and light irradiation for 180 min. The photocatalytic activity of the Ag/AC-ZnO was evaluated for the breakdown of BPA in a study by (Intarasuwan *et al.* 2018) under visible light irradiation. The results showed that Ag/AC-ZnO demonstrates more photocatalytic activity than AC-ZnO and pure ZnO. According to (Chen *et al.* 2017c), reduced graphene oxide encapsulates AgBr, creating a composite known as AgBr@rGO that may be introduced into graphene to create hydrogels with 3D network topologies (rGH-AgBr@rGO). When exposed to light, the 3D graphene nanosheets of rGH-AgBr@rGO quickly absorbed BPA. They swiftly decomposed to AgBr@rGO nanoparticles, proving the synergy between adsorption and photocatalytic degradation may greatly increase pollutant removal efficiency. Therefore, synergistic mechanisms produce better outcomes than other techniques, making them a promising strategy for eliminating EDCs. The integrated approach results for BPs removal are outlined in Table 4.

5. A SUMMARY OF THE MOST PREVALENT BPS ADSORPTION PARAMETERS

5.1. Adsorption isotherms

The sorption isotherm represents the sorption rate (q_e) versus concentration at equilibrium (Ce). It is common to use the Langmuir, Freundlich, Tempkin, and Dubinin Radshkevich (D-R) isotherm to describe the equilibrium behaviour of the adsorption process (Qayoom *et al.* 2017).

Table 4 | Synergetic removal of BPs

Carbon-based nanocomposites	Pollutants	Initial concentration (mg/L)	Dosage	Removal efficiency, %	Adsorption capacity (mg/g)	Light intensity	Contact time (min)	References
Ag/AC-ZnO	BPA	5	0.3 g	99.64	–	UV visible light	180	Intarasuwan *et al.* (2018)
(MOF) PCN-222	BPA	250	1 mg	86.8	487.69 ± 8.37	Visible light	20	Meng *et al.* (2017)
Nano Fe_3O_4-biochar/ peroxymonosulphate	BPA	20	2 g	100	–	–	90	Cui *et al.* (2021)
TiO_2-graphene hydrogel	BPA	20	–	62.4	476.2	Transient photocurrent response	240	Zhang *et al.* (2018)
TiO_2-MoS_2-rGo	BPA	10	0.5 g	62.4	–	UV Lamp	120	Luo *et al.* (2017)
CNTs with poplar leaves	BPA	10	10 mg	74	19.7	Solar simulator, 150 w xenon	180	Qu *et al.* (2012)
Graphene hydrogel-AgBr@rGO	BPA	20	0.1 g	91	80.1	400-W metal halide lamp	30	Chen *et al.* (2017a)
P(hea-co-ham)-cds	BPA	20	0.5 g	92	11.26	500 w xenon lamp	180	Zhu *et al.* (2018)

Where q_e and C_e indicate the amount mg of the adsorbed species per unit mass (g) of the composite adsorbent, the concentration of the species retained in solution, also, K_L and q_m are the model constant of Langmuir isotherm related with the affinity of active sites on the adsorbent's surface equilibrium, identified as the maximum adsorption capacity of the adsorbent. Another parameter described by the Langmuir model is the dimensionless factor of RL, which is called the separation factor and is defined by Equation (14):

$$RL = \frac{1}{1 + b.C_0} \tag{14}$$

C_0 is the initial metal ion concentration (mg/L), and b is the Langmuir constant. The absorption process will be unfavourable, favourable and linear, favourable and reversible, and irreversible for $RL > 1$, $RL = 1$, and $RL = 0$. The parameters K_f (mg/g) and n in the non-linear Freundlich equation are described as adsorption capacity and heterogeneity. The Tempkin isotherm denotes that the K_T and b are the Temkin isotherm equilibrium binding constant, Temkin constant, for the D-R isotherm, ε and β represent the Polanyi potential and activity coefficient, respectively (Clara *et al.* 2004). Table 2 lists numerous adsorbents studied for BP adsorption isotherms, including carbon-based materials, nanocomposites, agricultural waste, AC, and surfactant-modified adsorbents. Among various isotherms, Langmuir isotherm is the most widely observed because it is one of the simplest adsorption isotherms accurately characterized by several real-time systems. Several commercial adsorbents have uneven surfaces that favour adsorption at a particular spot. This explains that the adsorbate affinity is equal at all sites, with no adsorbate transmigration in the surface plane. Each molecule possesses sorption activation energy and constant enthalpies with no steric hindrance or lateral contact between the adsorbed molecules (Table 5) (Al-Ghouti & Da'ana 2020).

5.2. Adsorption kinetics

Adsorption kinetics are studied by looking at the adsorbent's change in adsorptive capacity or adsorptive rate (Singh *et al.* 2017). Table 6 shows the most often used kinetic models using linear and nonlinear equations for BPs removal (Zafar *et al.* 2015).

Where qe and q represent the adsorption capacities (mg/g) at equilibrium time with time t (h), k_1 is the pseudo-first-order model rate constant (h), k_2 (g/mg. h) is the rate adsorption constant, q_e (mg/g) represents the equilibrium adsorption capacity, q_t (mg/g) represents the amount adsorbed at time t. The slope and intercept of the plot (qt vs. $t^{1/2)}$ determine the k_p (mg/g/

Table 5 | The linear and nonlinear equations in isothermal models

Models	Linear equation	Non-linear equation	Mechanism
Langmuir	$C_e/q_e = 1/q_m\ (C_e) + 1/q_m\ K_L$	$q_e = q_m K_L C_e/(1 + K_L C_e)$	When no interaction between adsorbed species occurs, adsorption primarily consists of a monolayer at the surface and a homogenous site.
Freundlich	$\ln q_e = \ln k_F = 1/n\ (\ln C_e)$	$q_e = K_f\ C_e^{1/n}$	Based on the adsorbate adsorbed on the heterogeneous surface adsorption, this applies to both monolayer and multilayer adsorption.
Temkin	$q_e = RT/b(\ln k_T) + RT/b\ (\ln C_e)$	$q_e = RT/b_T\ \ln (K_T\ C_e)$	The Temkin isotherm model implies that all molecules' adsorption heat reduces linearly with increasing adsorbent surface coverage and that adsorption is characterized by a uniform distribution of binding energies up to a maximum acute point.
D-R	$\ln q_e = \ln q_m - \beta\varepsilon^2$	$q_e = q_m\ \exp (-\beta\varepsilon^2)$	According to the (D-R) isotherm model, adsorbent size is equivalent to micropore size, and the adsorption equilibrium relation for a particular adsorbate-adsorbent combination may be represented independent of temperature using the adsorption potential.

Table 6 | Kinetic relations between linear and non-linear

Models	Linear Equation	Non-linear equation	Mechanism
Pseudo first-order	$ln(q_e - q_t) = lnq_e - k_{1//}2.303.t$	$qt = qe[1 - e^{-k_1 t})]$	Physisorption limits the adsorption rate of the particles onto the adsorbent. The rate of adsorption site occupancy is related to the number of vacant sites on the adsorbent.
Pseudo second-order	$t/q_t = (1/k_2 q_e^2) + 1/q_e t)^2$	$qt = q_e^2 k_2 t/(1 + q_e k_2 t)$	It relates to the chemisorption process. The quantity of active surface sites and adsorbate ions on the adsorbent's surface determines the adsorption rate.
Intraparticle diffusion model	$q_t = k_p t^{(1/2)} + C$	$q_t = k_p t^{(1/2)}$	An intraparticle diffusion rate parameter has been used to describe the diffusion rate after the initial adsorption stages. The rate parameter has been calculated using several variables, including adsorbent mass, initial concentration, and particle size.
Elovich	$q_t = \beta ln(t) + \beta ln(\alpha)$	$q_t = 1/\beta.ln(1 + \alpha\beta)$	With more advanced adsorption, the reaction rate falls exponentially.

min) and C rate constants, β which reveal the adsorption constant (mg/g) throughout every experiment, the q_t shows the concentration of the solute adsorbed at time t, α and the speed constant (mg/g/min). Table 2 depicts the sorption process utilizing practically all adsorbents, which is the pseudo-second-order kinetic model. This is because pseudo-second-order (PSO) applies throughout a prolonged duration. In contrast, the pseudo-first-order (PFO) only applies to the beginning stage of the adsorption process (Hubbe *et al.* 2019). Fe_3O_4 magnetic nanoparticles (MNPs) were used to break down BPA, which was investigated by (Huang *et al.* 2012). With 15 min of contact time, the BPA was removed, usually occurring under all pH levels and following a pseudo-first-order kinetic response. With an R^2 of 0.99, the PSO model was to be optimal for the sorption process, demonstrating that the chemisorption interaction between the active sites on the adsorbent and the BPA anion is the primary source of adsorption. Using a co-precipitation technique (Zhang *et al.* 2014) they prepared reduced graphene oxide (rGO) nanosheets with MNPs. The equilibrium is reached between 4 and 6 h of contact time, which follows PSO, implying that sorption relies on the quantity of solute adsorbed on the adsorbent's surface and the amount adsorbed at equilibrium. Zhou *et al.* (2013) investigated the process of binding metal-organic framework adsorbents for BPA removal. The BPA molecules get diffused to the sorbent's outer surfaces before crossing the boundary layer and entering the cover. After entering the microporous framework was created by terephthalic acid with Al ions by intra-particle diffusion, BPA molecules were finally eliminated by reacting with the benzene ring and Al-OH on the sorbents. Therefore, whereas intra-particle diffusion is crucial near the end of the sorption, boundary layer diffusion governs the sorption rate of sorption in the beginning phase. So, it concludes that the metal-organic framework for BPA removal exhibits an intra-particle diffusion model. To

characterize chemical adsorption mechanisms in nature. Wu *et al.* (2009) explained the Elovich equation frequently employed in adsorption kinetics. Here, the adsorption kinetics characteristic curves were described using the Elovich equation (RE) equilibrium parameter.

5.3. Thermodynamics studies

Thermodynamic investigations give information regarding adsorption spontaneity and the nature of adsorbent and adsorbate under equilibrium circumstances. Moreover, thermodynamics provides knowledge identifying whether the adsorption process is favourable or unfavourable in a specified temperature range (Anastopoulos *et al.* 2018). Changes in Gibbs free energy (G), enthalpy (H), and entropy (S) are some of the factors used to forecast adsorption process characteristics (Tamjidi *et al.* 2021).

$$\Delta G^0 = -RTLnK_{th} \tag{15}$$

where R is the global gas constant (8.314 J/mol. K), T is the absolute temperature (K), and K_{th} is the equilibrium constant obtained.

$$K_{th} = q_e C_e \tag{16}$$

The graph of LnK_{th} vs. $1/T$ can be used to calculate the parameters H and S.

$$LnK_{th} = -\frac{\Delta G^0}{RT} = -\frac{\Delta H}{RT} = -\frac{\Delta H^0}{RT} + \frac{\Delta S^0}{R} \tag{17}$$

ΔG^0 at various temperatures indicates the feasibility of the process and the spontaneous nature of the adsorption. However, the negativity of ΔG^0 decreases with the increase in temperature, which suggested that the sequestration of adsorbate by adsorbent is unfavourable at elevated temperature. Negative G^0 and H^0 values indicate that the absorption process is feasible and exothermic. Also, a negative ΔS^0 value shows that the irregularity of the solid/solution interface is reduced. ΔG^0 at various temperatures, indicating the viability of the method and the spontaneous nature of the adsorption. Yet, the negative of ΔG^0 reduces as the temperature rises. This revealed that adsorbate sequestration by adsorbent is unfavourable at increased temperatures (Heiba *et al.* 2018). Table 7 summarizes recent thermodynamic studies on BPs removal with various adsorbents. According to Table 7, almost all adsorbents have negative H and G values, implying that the sorption mechanism is

Table 7 | Thermodynamic parameters for BPs elimination utilized in numerous research

Adsorbent	Pollutants	Temperature (°C)	ΔG° (kJ/mol)	ΔH° (kJ/mol)	ΔS° (J/mol. K)	References
Palm shell	BPA	29 ± 1	−2.5441	−3.9425	−4.615	Soni & Padmaja (2014)
		39.85	−2.498			
		49 ± 1	−2.4518			
		59.85	−2.4057			
Bentonite by HDTMA	BPA	19 ± 1	52,52	−2.9	−0.05	Genc *et al.* (2019)
		30	43.5			
		50	28.83			
		60	34.5			
MWCNTs	BPF	12 ± 1	−3.625	−16.621	−45.726	Zhang *et al.* (2013)
		24 ± 1	−2.836			
		39 ± 1	−2.387			
Fe/OMC	BPA	24 ± 1	−3.93	−20.84	−56.74	Tang *et al.* (2016)
		29 ± 1	−3.36			
		44 ± 1	−2.8			

exothermic and spontaneous. As the temperature rises, the adsorption process's efficiency will decrease, and it provides E_a negative value by using Equations (14)–(16). The negative activation energy in sorption processes exhibits exothermic nature and occurs at lower temperatures. The endothermic nature implies that adsorbate species become more soluble as temperature rises. As a result, the adsorbate is harder to adsorb because the forces of interaction between the adsorbate and solvent are more significant than those between the adsorbate and adsorbent (Lombardo *et al.* 2019).

6. COST ANALYSIS

The cost per mass of the raw materials used in the synthesis process is the factor that determines whether an adsorbent build is economically viable. This can be calculated using the cost of raw materials, amortized cash flow, the cost of adsorbent per gram of adsorbate removed, annual investment and operating expenditures (CAPEX and OPEX), and the cost of the adsorbent use in an adsorption process (Ighalo *et al.* 2022).

The adsorbent raw materials are made from agricultural waste, nanomaterials, clays, graphene polymer materials, and ACs. Whereas commercially available ACs are more expensive than ACs prepared from agricultural waste materials.

7. CONCLUSION

Water contamination caused by toxic BPs has become one of the world's foremost significant environmental concerns. Several intriguing treatments for removing BPs from aqueous systems have been established, including adsorption, photocatalytic degradation, electrochemical approaches, and membrane technologies. Although there are several options for treating BPs, each has positive and negative impacts. Adsorption and photocatalysis have much potential in water treatment applications regarding cost-effectiveness and sustainable development. Adsorption techniques have been comprehensively investigated using low-cost adsorbents, surfactant-modified adsorbents, carbon-based adsorbents, and biological adsorbents. Several photocatalytic degradation support mechanisms have been studied for the eradication of BPs. Furthermore, it was reported that an adsorption-photocatalysis synergetic technique might significantly reduce BPs in wastewater compared to an individual approaches. Overall, the optimum ratio composite exhibits good adsorption and photocatalytic activity. This article reviewed the effectiveness and significance of adsorption, photocatalytic degradation, and the synergy between the two treatment methods for removing EDCs from aqueous environment. Although these methods can treat BP's effluent, the appropriate one depends on several factors, notably the initial concentration, financial investment, industrial performance, maintenance cost, and ecological impact (Massoud *et al.* 2009).

DATA AVAILABILITY STATEMENT

All relevant data are included in the paper or its Supplementary Information.

CONFLICT OF INTEREST

The authors declare there is no conflict.

REFERENCES

Ahamad, T., Naushad, M., Ruksana, Alhabarah, A. N. & Alshehri, S. M. 2019 N/S doped highly porous magnetic carbon aerogel derived from sugarcane bagasse cellulose for the removal of bisphenol-A. *International Journal of Biological Macromolecules* **132**, 1031–1038. Available from: https://pubmed.ncbi.nlm.nih.gov/30951780/ (accessed 27 April 2023).

Ahmed, N., Vione, D., Rivoira, L., Carena, L., Castiglioni, M. & Bruzzoniti, M. C. 2021 A review on the degradation of pollutants by Fenton-like systems based on zero-valent iron and persulfate: effects of reduction potentials, pH, and anions occurring in waste waters. *Molecules (Basel, Switzerland)* **26** (15). Available from: https://pubmed.ncbi.nlm.nih.gov/34361737/ (accessed 2 May 2023).

Ahsan, M. A., Islam, M. T., Hernandez, C., Kim, H., Lin, Y., Curry, M. L., Gardea-Torresdey, J. & Noveron, J. C. 2018a Adsorptive removal of sulfamethoxazole and bisphenol A from contaminated water using functionalized carbonaceous material derived from tea leaves. *Journal of Environmental Chemical Engineering* **6** (4), 4215–4225.

Ahsan, M. A., Islam, M. T., Imam, M. A., Hyder, A. H. M. G., Jabbari, V., Dominguez, N. & Noveron, J. C. 2018b Biosorption of bisphenol A and sulfamethoxazole from water using sulfonated coffee waste: isotherm, kinetic and thermodynamic studies. *Journal of Environmental Chemical Engineering* **6** (5), 6602–6611.

Akgül, S., Sur, Ü., Düzçeker, Y., Balcı, A., Kızılkan, M. P., Kanbur, N., Bozdağ, G., Erkekoğlu, P., Gümüş, E., Kocer-Gumusel, B. & Derman, O. 2019 Bisphenol A and phthalate levels in adolescents with polycystic ovary syndrome. *Gynecological Endocrinology* **35** (12), 1084–1087.

Al-Ghouti, M. A. & Da'ana, D. A. 2020 Guidelines for the use and interpretation of adsorption isotherm models: a review. *Journal of Hazardous Materials* **393**, 1–22.

Al-Musawi, T. J., Mengelizadeh, N., Ganji, F., Wang, C. & Balarak, D. 2022 Preparation of multi-walled carbon nanotubes coated with CoFe2O4 nanoparticles and their adsorption performance for bisphenol A compound. *Advanced Powder Technology* **33** (2), 1–12.

Alves, A. C. F., Antero, R. V. P., de Oliveira, S. B., Ojala, S. A. & Scalize, P. S. 2019 Activated carbon produced from waste coffee grounds for an effective removal of bisphenol-A in aqueous medium. *Environmental Science and Pollution Research* **26** (24), 24850–24862.

Anastopoulos, I., Margiotoudis, I. & Massas, I. 2018 The use of olive tree pruning waste compost to sequestrate methylene blue dye from aqueous solution. *International Journal of Phytoremediation* **20** (8), 831–838.

Anglada, Á., Urtiaga, A. & Ortiz, I. 2009 Contributions of electrochemical oxidation to waste-water treatment: fundamentals and review of applications. *Journal of Chemical Technology and Biotechnology* **84** (12), 1747–1755.

Aragaw, T. A. 2021 The macro-debris pollution in the shorelines of Lake Tana: first report on abundance, assessment, constituents, and potential sources. *Science of the Total Environment* **797**, 1–10.

Aretoulaki, E., Ponis, S., Plakas, G. & Agalianos, K. 2020 *A* systematic meta-review analysis of review papers in the marine plastic pollution literature. *Marine Pollution Bulletin* **161**, 1–10.

Bahadoran, A., Najafizadeh, M., Liu, Q., De Lile, J. R., Zhang, D., Masudy-Panah, S., Ramakrishna, S., Fakhri, A. & Gupta, V. K. 2021 Co-doping silver and iron on graphitic carbon nitride-carrageenan nanocomposite for the photocatalytic process, rapidly colorimetric detection and antibacterial properties. *Surfaces and Interfaces* **26**, 1–9.

Balarak, D., Mostafapour, F. K., Lee, S. M. & Jeon, C. 2019 Adsorption of bisphenol A using dried rice husk: equilibrium, kinetic and thermodynamic studies. *Applied Chemistry for Engineering* **30** (3), 316–323. https://doi.org/10.14478/ace.2019.1013. (accessed 27 April 2023).

Balci, B. & Erkurt, F. E. 2017 Adsorption of bisphenol-A by eucalyptus bark/magnetite composite: modeling the effect of some independent parameters by multiple linear regression. *Adsorption Science and Technology* **35** (3–4), 339–356.

Barnes, D. K. A., Galgani, F., Thompson, R. C. & Barlaz, M. 2009 Accumulation and fragmentation of plastic debris in global environments. *Philosophical Transactions of the Royal Society B: Biological Sciences* **364** (1526), 1985–1998.

Barquilha, C. E. R. & Braga, M. C. B. 2021 Adsorption of organic and inorganic pollutants onto biochars: challenges, operating conditions, and mechanisms. *Bioresource Technology Reports* **15**, 1–15.

Bechambi, O., Chalbi, M., Najjar, W. & Sayadi, S. 2015 Photocatalytic activity of ZnO doped with Ag on the degradation of endocrine disrupting under UV irradiation and the investigation of its antibacterial activity. *Applied Surface Science* **347**, 414–420.

Belhaj, A. F., Elraies, K. A., Mahmood, S. M., Zulkifli, N. N., Akbari, S. & Hussien, O. S. E. 2020 The effect of surfactant concentration, salinity, temperature, and pH on surfactant adsorption for chemical enhanced oil recovery: a review. *Journal of Petroleum Exploration and Production Technology* **10** (1), 125–137.

Bhadra, B. N., Lee, J. K., Cho, C. W. & Jhung, S. H. 2018 Remarkably efficient adsorbent for the removal of bisphenol A from water: Bio-MOF-1-derived porous carbon. *Chemical Engineering Journal* **343**, 225–234.

Bhatia, D. & Datta, D. 2019 Removal of bisphenol-A using amine-modified magnetic multiwalled carbon nanotubes: batch and column studies. *Journal of Chemical and Engineering Data* **64** (6), 2877–2887.

Biber, N. F. A., Foggo, A. & Thompson, R. C. 2019 Characterising the deterioration of different plastics in air and seawater. *Marine Pollution Bulletin* **141**, 1–21.

Blinová, L. & Sirotiak, M. 2021 Utilization of waste-based sorbents for removal of pharmaceuticals from water: a review. *Research Papers Faculty of Materials Science and Technology Slovak University of Technology* **29** (48), 22–36.

Born, M. P. & Brüll, C. 2022 From model to nature – a review on the transferability of marine (micro-) plastic fragmentation studies. *Science of the Total Environment* **811**, 1–12.

Bousoumah, R., Leso, V., Iavicoli, I., Huuskonen, P., Viegas, S., Porras, S. P., Santonen, T., Frery, N., Robert, A. & Ndaw, S. 2021 Biomonitoring of occupational exposure to bisphenol A, bisphenol S and bisphenol F: a systematic review. *Science of the Total Environment* **783**, 1–11.

Brandsma, S. H., Leonards, P. E. G., Koekkoek, J. C., Samsonek, J. & Puype, F. 2022 Migration of hazardous contaminants from WEEE contaminated polymeric toy material by mouthing. *Chemosphere* **294**, 1–9.

Chang, K. L., Hsieh, J. F., Ou, B. M., Chang, M. H., Hseih, W. Y., Lin, J. H., Huang, P. J., Wong, K. F. & Chen, S. T. 2012 Adsorption studies on the removal of an endocrine-disrupting compound (Bisphenol A) using activated carbon from rice straw agricultural waste. *Separation Science and Technology (Philadelphia)* **47** (10), 1514–1521.

Chen, M., Ohman, K., Metcalfe, C., Ikonomou, M. G., Amatya, P. L. & Wilson, J. 2006 Pharmaceuticals and endocrine disruptors in wastewater treatment effluents and in the water supply system of Calgary, Alberta, Canada. *Water Quality Research Journal of Canada* **41** (4), 351–364.

Chen, D., Kannan, K., Tan, H., Zheng, Z., Feng, Y. L., Wu, Y. & Widelka, M. 2016a Bisphenol analogues other than BPA: environmental occurrence, human exposure, and toxicity – a review. *Environmental Science and Technology* **50** (11), 5438–5453.

Chen, Z., Jiang, H., Jin, W. & Shi, C. 2016b Enhanced photocatalytic performance over Bi4Ti3O12 nanosheets with controllable size and exposed {001} facets for rhodamine B degradation. *Applied Catalysis B: Environmental* **180**, 698–706.

Chen, F., An, W., Liu, L., Liang, Y. & Cui, W. 2017a Highly efficient removal of bisphenol A by a three-dimensional graphene hydrogel-AgBr@rGO exhibiting adsorption/photocatalysis synergy. *Applied Catalysis B: Environmental* **217**, 65–80.

Chen, F., Gao, W., Qiu, X., Zhang, H., Liu, L., Liao, P., Fu, W. & Luo, Y. 2017b Graphene quantum dots in biomedical applications: recent advances and future challenges. *Frontiers in Laboratory Medicine* **1** (4), 192–199.

Chen, Q., Yin, D., Jia, Y., Schiwy, S., Legradi, J., Yang, S. & Hollert, H. 2017c Enhanced uptake of BPA in the presence of nano plastics can lead to neurotoxic effects in adult zebrafish. *Science of the Total Environment* **609**, 1312–1321.

Cheung, P. K. & Fok, L. 2017 Characterisation of plastic microbeads in facial scrubs and their estimated emissions in Mainland China. *Water Research* **122**, 53–61.

Chiriac, F. L., Pirvu, F. & Paun, I. 2021 Investigation of endocrine disruptor pollutants and their metabolites along the Romanian Black Sea coast: occurrence, distribution and risk assessment. *Environmental Toxicology and Pharmacology* **86**, 1–11.

Chu, G., Zhao, J., Chen, F., Dong, X., Zhou, D., Liang, N., Wu, M., Pan, B. & Steinberg, C. E. W. 2017 Physi-chemical and sorption properties of biochars prepared from peanut shell using thermal pyrolysis and microwave irradiation. *Environmental Pollution* **227**, 372–379.

Clara, M., Strenn, B., Saracevic, E. & Kreuzinger, N. 2004 Adsorption of bisphenol-A, 17β-estradiole and 17α- ethinylestradiole to sewage sludge. *Chemosphere* **56** (9), 843–851.

Cooper, J. E., Kendig, E. L. & Belcher, S. M. 2011 Assessment of bisphenol A released from reusable plastic, aluminium and stainless–steel water bottles. *Chemosphere* **85** (6), 943–947.

Crini, G. 2005 Recent developments in polysaccharide-based materials used as adsorbents in wastewater treatment. *Progress in Polymer Science (Oxford)* **30** (1), 38–70.

Cui, X., Zhang, S. S., Gen, Y., Zhen, J., Zhan, J., Cao, C. & Ni, S. Q. 2021 Synergistic catalysis by Fe3O4-biochar/peroxymonosulfate system for the removal of bisphenol A. *Separation and Purification Technology* **276**, 1–8.

Debroy, A., George, N. & Mukherjee, G. 2022 Role of biofilms in the degradation of microplastics in aquatic environments. *Journal of Chemical Technology and Biotechnology* **97** (12), 3271–3282.

Dehghani, M. H., Sanaei, D., Ali, I. & Bhatnagar, A. 2016 Removal of chromium(VI) from aqueous solution using treated waste newspaper as a low-cost adsorbent: kinetic modeling and isotherm studies. *Journal of Molecular Liquids* **215**, 671–679.

De Gisi, S., Lofrano, G., Grassi, M. & Notarnicola, M. 2016 Characteristics and adsorption capacities of low-cost sorbents for wastewater treatment: a review. *Sustainable Materials and Technologies* **9**, 10–40.

de Siqueira, C. D., Adenrele, A. O., de Moraes, A. C. R. & Filippin-Monteiro, F. B. 2023 Human body burden of bisphenol A: a case study of lactating mothers in Florianopolis, Brazil. *Environmental Science and Pollution Research* **30** (1), 1785–1794.

Dovi, E., Kani, A. N., Aryee, A. A., Jie, M., Li, J., Li, Z., Qu, L. & Han, R. 2021 Decontamination of bisphenol A and Congo red dye from solution by using CTAB functionalised walnut shell. *Environmental Science and Pollution Research International* **28** (22), 28732–28749. Available from: https://pubmed.ncbi.nlm.nih.gov/33550551/ (accessed 2 May 2023).

Duan, F., Chen, C., Chen, L., Sun, Y., Wang, Y., Yang, Y., Liu, X. & Qin, Y. 2014 Preparation and evaluation of water-compatible surface molecularly imprinted polymers for selective adsorption of bisphenol a from aqueous solution. *Industrial and Engineering Chemistry Research* **53** (37), 14291–14300.

Duan, C., Ma, T., Wang, J. & Zhou, Y. 2020 Removal of heavy metals from aqueous solution using carbon-based adsorbents: a review. *Journal of Water Process Engineering* **37**, 1–13.

Eaton, C. J., Coxon, S., Pattis, I., Chappell, A., Hewitt, J. & Gilpin, B. J. 2022 A framework for public health authorities to evaluate health determinants for wastewater–based epidemiology. *Environmental Health Perspectives* **130** (12), 125001 (1–9).

Fang, Z., Hu, Y., Wu, X., Qin, Y., Cheng, J., Chen, Y., Tan, P. & Li, H. 2018 A novel magnesium ascorbyl phosphate graphene-based monolith and its superior adsorption capability for bisphenol A. *Chemical Engineering Journal* **334**, 948–956.

Fang, W., Peng, Y., Muir, D., Lin, J. & Zhang, X. 2019 A critical review of synthetic chemicals in surface waters of the US, the EU and China. *Environment International* **131**, 1–11.

Ferdous, R. M., Reza, A. W. & Siddiqui, M. F. 2016 Renewable energy harvesting for wireless sensors using passive RFID tag technology: a review. *Renewable and Sustainable Energy Reviews* **58**, 1114–1128.

Fomina, M. & Gadd, G. M. 2014 Biosorption: current perspectives on concept, definition and application. *Bioresource Technology* **160**, 3–14.

Fotopoulou, K. N. & Karapanagioti, H. K. 2019 Degradation of various plastics in the environment. *Hazardous Chemicals Associated with Plastics in the Marine Environment*, 71–92.

Fromme, H., Küchler, T., Otto, T., Pilz, K., Müller, J. & Wenzel, A. 2002 Occurrence of phthalates and bisphenol A and F in the environment. *Water Research* **36** (6), 1429–1438.

Genc, N., Durna, E. & Kilicoglu, O. 2019 Removal of bisphenol from aqueous solution by surfactant-modified bentonite. *Journal of Water Chemistry and Technology* **41** (4), 236–241.

Gnanaprakasam, A., Sivakumar, V. M. & Thirumarimurugan, M. 2015 Influencing parameters in the photocatalytic degradation of organic effluent via nanometal oxide catalyst: a review. *Indian Journal of Materials Science* **2015**, 1–16.

Gore, A. C., Chappell, V. A., Fenton, S. E., Flaws, J. A., Nadal, A., Prins, G. S., Toppari, J. & Zoeller, R. T. 2015 Executive summary to EDC-2: the endocrine society's second scientific statement on endocrine-disrupting chemicals. *Endocrine Reviews* **36** (6), 593–602. Available from: https://www.researchgate.net/publication/282514965_Executive_Summary_to_EDC-2_The_Endocrine_Society's_Second_Scientific_Statement_on_Endocrine-Disrupting_Chemicals (accessed 26 April 2023).

Goyal, N., Barman, S. & Bulasara, V. K. 2018 Efficient removal of bisphenol S from aqueous solution by synthesized nano-zeolite secony Mobil-5. *Microporous and Mesoporous Materials* **259**, 184–194.

Gunaalan, K., Fabbri, E. & Capolupo, M. 2020 The hidden threat of plastic leachates: a critical review on their impacts on aquatic organisms. *Water Research* **184**. Available from: https://pubmed.ncbi.nlm.nih.gov/32698093/ (accessed 25 April 2023).

Guo, W., Hu, W., Pan, J., Zhou, H., Guan, W., Wang, X., Dai, J. & Xu, L. 2011 Selective adsorption and separation of BPA from aqueous solution using novel molecularly imprinted polymers based on kaolinite/Fe3O4 composites. *Chemical Engineering Journal* **171** (2), 603–611.

Guo, X., Huang, Y., Yu, W., Yu, X., Han, X. & Zhai, H. 2020 Multi-walled carbon nanotubes modified with iron oxide and manganese dioxide (MWCNTs-Fe3O4 – MnO2) as a novel adsorbent for the determination of BPA. *Microchemical Journal* **157**, 1–10.

Hacıosmanoğlu, G. G., Doğruel, T., Genç, S., Oner, E. T. & Can, Z. S. 2019 Adsorptive removal of bisphenol A from aqueous solutions using phosphonated levan. *Journal of Hazardous Materials* **374**, 43–49.

Hamadeen, H. M. & Elkhatib, E. A. 2022 New nanostructured activated biochar for effective removal of antibiotic ciprofloxacin from wastewater: adsorption dynamics and mechanisms. *Environmental Research* **210**, 1–11.

Hartono, M. R., Assaf, A., Thouand, G., Kushmaro, A., Chen, X. & Marks, R. S. 2015 Use of bamboo powder waste for removal of bisphenol A in aqueous solution. *Water, Air, and Soil Pollution* **226** (11), 1–11.

Heiba, H. F., Taha, A. A., Mostafa, A. R., Mohamed, L. A. & Fahmy, M. A. 2018 Synthesis and characterization of CMC/MMT nanocomposite for Cu2 + sequestration in wastewater treatment. *Korean Journal of Chemical Engineering* **35** (9), 1844–1853.

Heidarinejad, Z., Dehghani, M. H., Heidari, M., Javedan, G., Ali, I. & Sillanpää, M. 2020 Methods for preparation and activation of activated carbon: a review. *Environmental Chemistry Letters* **18** (2), 393–415. Available from: https://link.springer.com/article/10.1007/s10311-019-00955-0 (accessed 3 July 2023).

Hermabessiere, L., Dehaut, A., Paul-Pont, I., Lacroix, C., Jezequel, R., Soudant, P. & Duflos, G. 2017 Occurrence and effects of plastic additives on marine environments and organisms: a review. *Chemosphere* **182**, 781–793.

Hu, L., Zhang, G., Liu, M., Wang, Q. & Wang, P. 2018 Enhanced degradation of bisphenol A (BPA) by peroxymonosulfate with Co3O4-Bi2O3 catalyst activation: effects of pH, inorganic anions, and water matrix. *Chemical Engineering Journal* **338**, 300–310.

Huang, R., Fang, Z., Yan, X. & Cheng, W. 2012 Heterogeneous sono-Fenton catalytic degradation of bisphenol A by Fe3O4 magnetic nanoparticles under neutral condition. *Chemical Engineering Journal* **197**, 242–249.

Hubbe, M., Azizian, S. & Douven, S. 2019 Implications of apparent pseudo-second-order adsorption kinetics onto cellulosic materials: a review. *BioResources* **14** (3), 7582–7626. Available from: https://bioresources.cnr.ncsu.edu/resources/implications-of-apparent-pseudo-second-order-adsorption-kinetics-onto-cellulosic-materials-a-review/ (accessed 27 April 2023).

Huerta Lwanga, E., Mendoza Vega, J., Ku Quej, V., Chi, J. d. l. A., Sanchez del Cid, L., Chi, C., Escalona Segura, G., Gertsen, H., Salánki, T., van der Ploeg, M., Koelmans, A. A. & Geissen, V. 2017 Field evidence for transfer of plastic debris along a terrestrial food chain. *Scientific Reports* **7** (1), 1–7.

Ighalo, J. O., Omoarukhe, F. O., Ojukwu, V. E., Iwuozor, K. O. & Igwegbe, C. A. 2022 Cost of adsorbent preparation and usage in wastewater treatment: a review. *Cleaner Chemical Engineering* **3**, 100042.

Intarasuwan, K., Amornpitoksuk, P., Suwanboon, S., Graidist, P., Maungchanburi, S. & Randorn, C. 2018 Effect of Ag loading on activated carbon doped ZnO for bisphenol A degradation under visible light. *Advanced Powder Technology* **29** (11), 2608–2615.

Jamil, T. S. & Mansor, E. S. 2018 Enhancing photocatalytic performance of BiOX for bisphenol-A degradation. *Research Article* **2018** (3), 155–160. Available from: www.vbripress.com/amp (accessed 3 May 2023).

Jang, Y. C., Lee, G., Kwon, Y., Lim, J. H. & Jeong, J. H. 2020 Recycling and management practices of plastic packaging waste towards a circular economy in South Korea. *Resources, Conservation and Recycling* **158**, 1–11.

Javid, N. & Malakootian, M. 2017 Removal of bisphenol A from aqueous solutions by modified-carbonized date pits by ZnO nano-particles. Available from: www.deswater.com (accessed 3 May 2023).

Jin, H., Zhu, J., Chen, Z., Hong, Y. & Cai, Z. 2018 Occurrence and partitioning of bisphenol analogues in adults' blood from China. *Environmental Science and Technology* **52** (2), 812–820.

Jjagwe, J., Olupot, P. W., Menya, E. & Kalibbala, H. M. 2021 Synthesis and application of granular activated carbon from biomass waste materials for water treatment: a review. *Journal of Bioresources and Bioproducts* **6** (4), 292–322.

Joseph, L., Heo, J., Park, Y. G., Flora, J. R. V. & Yoon, Y. 2011 Adsorption of bisphenol A and 17α-ethinyl estradiol on single walled carbon nanotubes from seawater and brackish water. *Desalination* **281** (1), 68–74.

Kalderis, D., Koutoulakis, D., Paraskeva, P., Diamadopoulos, E., Otal, E., Valle, J. O. d. & Fernández-Pereira, C. 2008 Adsorption of polluting substances on activated carbons prepared from rice husk and sugarcane bagasse. *Chemical Engineering Journal* **144** (1), 42–50.

Kanan, S., Moyet, M. A., Arthur, R. B. & Patterson, H. H. 2020 Recent advances on TiO2-based photocatalysts toward the degradation of pesticides and major organic pollutants from water bodies. *Catalysis Reviews – Science and Engineering* **62** (1), 1–65.

Kasonga, T. K., Coetzee, M. A. A., Kamika, I., Ngole-Jeme, V. M. & Benteke Momba, M. N. 2021 Endocrine-disruptive chemicals as contaminants of emerging concern in wastewater and surface water: a review. *Journal of Environmental Management* **277**. Available from: https://pubmed.ncbi.nlm.nih.gov/33049614/ (accessed 26 April 2023).

Katančić, Z., Chen, W. T., Waterhouse, G. I. N., Kušić, H., Lončarić Božić, A., Hrnjak-Murgić, Z. & Travas-Sejdic, J. 2020 Solar-active photocatalysts based on TiO2 and conductive polymer PEDOT for the removal of bisphenol A. *Journal of Photochemistry and Photobiology A: Chemistry* **396**, 1–7.

Koduru, J. R., Lingamdinne, L. P., Singh, J. & Choo, K. H. 2016 Effective removal of bisphenol-A (BPA) from water using a goethite/activated carbon composite. *Process Safety and Environmental Protection* **103**, 87–96.

Kuang, Y., Yang, R., Zhang, Z., Fang, J., Xing, M. & Wu, D. 2019 Surfactant-loaded graphene oxide sponge for the simultaneous removal of Cu2 + and bisphenol A from water. *Chemosphere* **236**, 1–9.

Kumar, A. 2017 A review on the factors affecting the photocatalytic degradation of hazardous materials. *Material Science & Engineering International Journal* **1** (3). Available from: https://www.researchgate.net/publication/321290906_A_Review_on_the_Factors_Affecting_the_Photocatalytic_Degradation_of_Hazardous_Materials (accessed 27 April 2023).

Kumar, J. & Bansal, A. 2013 Photocatalysis by nanoparticles of titanium dioxide for drinking water purification: a conceptual and state-of-art review. *Materials Science Forum* **764**, 130–150. Available from: https://www.researchgate.net/publication/258952571_Photocatalysis_by_Nanoparticles_of_Titanium_Dioxide_for_Drinking_Water_Purification_A_Conceptual_and_State-of-Art_Review (accessed 27 April 2023).

Lawal, I. A., Klink, M., Ndungu, P. & Moodley, B. 2019 Brief bibliometric analysis of 'ionic liquid' applications and its review as a substitute for common adsorbent modifier for the adsorption of organic pollutants. *Environmental Research* **175**, 34–51. Available from: https://www.researchgate.net/publication/332917932_Brief_bibliometric_analysis_of_ionic_liquid_applications_and_its_review_as_a_substitute_for_common_adsorbent_modifier_for_the_adsorption_of_organic_pollutants (accessed 27 April 2023).

Lazim, Z. M., Hadibarata, T., Puteh, M. H. & Yusop, Z. 2015 Adsorption characteristics of bisphenol a onto low-cost modified phyto-waste material in aqueous solution. *Water, Air, and Soil Pollution* **226** (3), 1–11.

Lebreton, L., Egger, M. & Slat, B. 2019 A global mass budget for positively buoyant macroplastic debris in the ocean. *Scientific Reports* **9** (1), 1–9.

Lechthaler, S., Schwarzbauer, J., Reicherter, K., Stauch, G. & Schüttrumpf, H. 2020a Regional study of microplastics in surface waters and deep sea sediments south of the Algarve Coast. *Regional Studies in Marine Science* **40**, 1–11.

Lechthaler, S., Waldschläger, K., Stauch, G. & Schüttrumpf, H. 2020b The way of macroplastic through the environment. *Environments – MDPI* **7** (10), 1–30.

Li, W., Li, D., Lin, Y., Wang, P., Chen, W., Fu, X. & Shao, Y. 2012 Evidence for the active species involved in the photodegradation process of methyl Orange on TiO2. *Journal of Physical Chemistry C* **116** (5), 3552–3560.

Li, J., Zhan, Y., Lin, J., Jiang, A. & Xi, W. 2014 Removal of bisphenol A from aqueous solution using cetylpyridinium bromide (CPB)-modified natural zeolites as adsorbents. *Environmental Earth Sciences* **72** (10), 3969–3980.

Li, W. C., Tse, H. F. & Fok, L. 2016 Plastic waste in the marine environment: a review of sources, occurrence and effects. *Science of the Total Environment* **566–567**, 333–349.

Li, J., Liang, N., Jin, X., Zhou, D., Li, H., Wu, M. & Pan, B. 2017 The role of ash content on bisphenol A sorption to biochars derived from different agricultural wastes. *Chemosphere* **171**, 66–73.

Lintelmann, J., Katayama, A., Kurihara, N., Shore, L. & Wenzel, A. 2003 Endocrine disruptors in the environment: (IUPAC technical report). *Pure and Applied Chemistry* **75** (5), 631–681.

Liu, X., Jin, A., Jia, Y., Xia, T., Deng, C., Zhu, M., Chen, C. & Chen, X. 2017 Synergy of adsorption and visible-light photocatalytic degradation of methylene blue by a bifunctional Z-scheme heterojunction of WO 3/g-C 3 N 4. *Applied Surface Science* **405**, 359–371.

Lombardo, S., Gençer, A., Schütz, C., Van Rie, J., Eyley, S. & Thielemans, W. 2019 Thermodynamic study of ion-driven aggregation of cellulose nanocrystals. *Biomacromolecules* **20** (8), 3181–3190.

Luo, L. J., Li, J., Dai, J., Xia, L., Barrow, C. J., Wang, H., Jegatheesan, J. & Yang, M. 2017 Bisphenol A removal on TiO2-mos2-reduced graphene oxide composite by adsorption and photocatalysis. *Process Safety and Environmental Protection* **112**, 274–279. Available from: https://researchrepository.rmit.edu.au/esploro/outputs/journalArticle/Bisphenol-A-removal-on-TiO2-MoS2-reduced-graphene/9921862955901341 (accessed 27 April 2023).

Lusher, A. L., Tirelli, V., O'Connor, I. & Officer, R. 2015 Microplastics in Arctic polar waters: the first reported values of particles in surface and sub-surface samples. *Scientific Reports* **5**, 1–9.

Luyckx, V. A., Al-Aly, Z., Bello, A. K., Bellorin-Font, E., Carlini, R. G., Fabian, J., Garcia-Garcia, G., Iyengar, A., Sekkarie, M., van Biesen, W., Ulasi, I., Yeates, K. & Stanifer, J. 2021 Sustainable development goals relevant to kidney health: an update on progress. *Nature Reviews Nephrology* **17** (1), 1–18.

Lv, Y., Liu, Y., Wei, J., Li, M., Xu, D. & Lai, B. 2021 Bisphenol S degradation by visible light assisted peroxymonosulfate process based on BiOI/B4C photocatalysts with Z-scheme heterojunction. *Chemical Engineering Journal* **417**, 129188.

Martín-Lara, M. A., Calero, M., Ronda, A., Iáñez-Rodríguez, I. & Escudero, C. 2020 Adsorptive behavior of an activated carbon for bisphenol A removal in single and binary (bisphenol A-heavy metal) solutions. *Water (Switzerland)* **12** (8), 1–20.

Massoud, M. A., Tarhini, A. & Nasr, J. A. 2009 Decentralized approaches to wastewater treatment and management: applicability in developing countries. *Journal of Environmental Management* **90** (1), 652–659.

Mei, P., Wang, H., Guo, H., Zhang, N., Ji, S., Ma, Y., Xu, J., Li, Y., Alsulami, H., Alhodaly, M. S., Hayat, T. & Sun, Y. 2020 The enhanced photodegradation of bisphenol A by TiO2/C3N4 composites. *Environmental Research* **182**, 1–7.

Meng, A. N., Chaihu, L. X., Chen, H. H. & Gu, Z. Y. 2017 Ultrahigh adsorption and singlet-oxygen mediated degradation for efficient synergetic removal of bisphenol A by a stable zirconium-porphyrin metal-organic framework. *Scientific Reports* **7** (1). Available from: https://pubmed.ncbi.nlm.nih.gov/28740182/ (accessed 27 April 2023).

Mhiret Gela, S. & Aragaw, T. A. 2022 Abundance and characterization of microplastics in main urban ditches across the Bahir Dar City, Ethiopia. *Frontiers in Environmental Science* **10**, 1–16.

Miriyam, I. B., Anbalagan, K. & Kumar, M. M. 2022 Phthalates removal from wastewater by different methods – a review. *Water Science and Technology* **85** (9), 2581–2600.

Moon, S., Yu, S. H., Lee, C. B., Park, Y. J., Yoo, H. J. & Kim, D. S. 2021 Effects of bisphenol A on cardiovascular disease: an epidemiological study using National Health and Nutrition Examination Survey 2003–2016 and meta-analysis. *Science of the Total Environment* **763**, 1–11.

Moreno-Castilla, C. 2004 Adsorption of organic molecules from aqueous solutions on carbon materials. *Carbon* **42** (1), 83–94.

Morin-Crini, N., Lichtfouse, E., Torri, G. & Crini, G. 2019 Applications of chitosan in food, pharmaceuticals, medicine, cosmetics, agriculture, textiles, pulp and paper, biotechnology, and environmental chemistry. *Environmental Chemistry Letters* **17** (4), 1667–1692.

Mühlberg, M. 2020 Retraction: recent advances of metal–metal oxide nanocomposites and their tailored nanostructures in numerous catalytic applications. *Journal of Materials Chemistry A* **8** (30), 15189–15189. Available from: https://pubs.rsc.org/en/content/articlehtml/2020/ta/d0ta90164d (accessed 3 May 2023).

Mundkur, N., Khan, A. S., Khamis, M. I., Ibrahim, T. H. & Nancarrow, P. 2022 Synthesis and characterization of clay-based adsorbents modified with alginate, surfactants, and nanoparticles for methylene blue removal. *Environmental Nanotechnology, Monitoring and Management* **17**, 1–11.

Naeemullah & Tuzen, M. 2019 Development of tetraethylene pentamine functionalized multi-wall carbon nanotubes as a new adsorbent in a syringe system for removal of bisphenol A by using multivariate optimization techniques. *Microchemical Journal* **147**, 1147–1154.

Naganathan, K. K., Faizal, A. N. M., Zaini, M. A. A. & Ali, A. 2021 Adsorptive removal of bisphenol a from aqueous solution using activated carbon from coffee residue. *Materials Today: Proceedings* **47**, 1307–1312.

Natarajan, S., Bajaj, H. C. & Tayade, R. J. 2018 Recent advances based on the synergetic effect of adsorption for removal of dyes from waste water using photocatalytic process. *Journal of Environmental Sciences (China)* **65**, 201–222.

Okan, M., Aydin, H. M. & Barsbay, M. 2019 Current approaches to waste polymer utilization and minimization: a review. *Journal of Chemical Technology and Biotechnology* **94** (1), 8–21.

Orimolade, B. O., Adekola, F. A. & Adebayo, G. B. 2018 Adsorptive removal of bisphenol A using synthesized magnetite nanoparticles. *Applied Water Science* **8** (1), 1–8.

Orona-Návar, C., Park, Y., Srivastava, V., Hernández, N., Mahlknecht, J., Sillanpää, M. & Ornelas-Soto, N. 2021 Gd3 + doped BiVO4 and visible light-emitting diodes (LED) for photocatalytic decomposition of bisphenol A, bisphenol S and bisphenol AF in water. *Journal of Environmental Chemical Engineering* **9** (5), 1–12.

Park, J. M. & Jhung, S. H. 2021 Remarkable adsorbent for removal of bisphenol A and S from water: porous carbon derived from melamine/polyaniline. *Chemosphere* **268**, 1–37.

Peng, L., Fu, D., Qi, H., Lan, C. Q., Yu, H. & Ge, C. 2020 Micro- and nano-plastics in marine environment: source, distribution and threats – a review. *Science of the Total Environment* **698**, 1–12.

Qayoom, A., Kazmi, S. A. & Ali, S. N. 2017 Equilibrium modelling for adsorption of aqueous Cd(II) onto turmeric: linear versus nonlinear regression analysis. *Moroccan Journal of Chemistry* **5** (2), 362–370. Available from: https://revues.imist.ma/index.php/morjchem/article/view/6548 (accessed 2 May 2023).

Qu, J., Cong, Q., Luo, C. & Yuan, X. 2012 Adsorption and photocatalytic degradation of bisphenol A by low-cost carbon nanotubes synthesized using fallen leaves of poplar. *RSC Advances* **3** (3), 961–965. Available from: https://pubs.rsc.org/en/content/articlehtml/2013/ra/c2ra21522e (accessed 27 April 2023).

Rajabi, H. R., Karimi, F., Kazemdehdashti, H. & Kavoshi, L. 2018 Fast sonochemically-assisted synthesis of pure and doped zinc sulfide quantum dots and their applicability in organic dye removal from aqueous media. *Journal of Photochemistry and Photobiology B: Biology* **181**, 98–105.

Rajmohan, K. V. S., Ramya, C., Raja Viswanathan, M. & Varjani, S. 2019 Plastic pollutants: effective waste management for pollution control and abatement. *Current Opinion in Environmental Science and Health* **12**, 72–84.

Rathi, B. S. & Kumar, P. S. 2021 Application of adsorption process for effective removal of emerging contaminants from water and wastewater. *Environmental Pollution* **280**. Available from: https://www.researchgate.net/publication/350333651_Application_of_Adsorption_Process_for_Effective_Removal_of_Emerging_Contaminants_from_Water_and_Wastewater (accessed 26 April 2023).

Rhodes, C. J. 2018 Plastic pollution and potential solutions. *Science Progress* **101** (3), 207–260.

RongChang, W., DianJun, R., SiQing, X., YaLei, Z. & JianFu, Z. 2009 Photocatalytic degradation of bisphenol A (BPA) using immobilized TiO2 and UV illumination in a horizontal circulating bed photocatalytic reactor (HCBPR). *Journal of Hazardous Materials* **169** (1/3), 926–932.

Sabzehmeidani, M. M., Mahnaee, S., Ghaedi, M., Heidari, H. & Roy, V. A. L. 2021 Carbon based materials: a review of adsorbents for inorganic and organic compounds. *Materials Advances* **2** (2), 598–627. Available from: https://pubs.rsc.org/en/content/articlehtml/2021/ma/d0ma00087f (accessed 28 April 2023).

Sadegh, H. & Ali, G. A. M. 2018 Potential applications of nanomaterials in wastewater treatment. June, 51–61.

Sahu, R. S., Shih, Y. H. & Chen, W. L. 2021 New insights of metal free 2D graphitic carbon nitride for photocatalytic degradation of bisphenol A. *Journal of Hazardous Materials* **402**, 1–9.

Santhi, V. A., Sakai, N., Ahmad, E. D. & Mustafa, A. M. 2012 Occurrence of bisphenol A in surface water, drinking water and plasma from Malaysia with exposure assessment from consumption of drinking water. *Science of the Total Environment* **427–428**, 332–338. Available from: https://www.researchgate.net/publication/224947964_Occurrence_of_Bisphenol_A_in_Surface_Water_Drinking_Water_and_Plasma_from_Malaysia_with_Exposure_Assessment_from_Consumption_of_Drinking_Water (accessed 26 April 2023).

Saxena, R., Saxena, M. & Lochab, A. 2020 Recent progress in nanomaterials for adsorptive removal of organic contaminants from wastewater. *ChemistrySelect* **5** (1), 335–353.

Schiffmann, R. 2017 Packaging for microwave foods. In: *The Microwave Processing of Foods: Second Edition*. Woodhead Publishing, Cambridge, UK, pp. 273–299.

Schmaltz, E., Melvin, E. C., Diana, Z., Gunady, E. F., Rittschof, D., Somarelli, J. A., Virdin, J. & Dunphy-Daly, M. M. 2020 Plastic pollution solutions: emerging technologies to prevent and collect marine plastic pollution. *Environment International* **144**, 1–17.

Şenol, Z. M., Gül, Ü. D. & Gürkan, R. 2020 Bio-sorption of bisphenol a by the dried- and inactivated-lichen (Pseudoevernia furfuracea) biomass from aqueous solutions. *Journal of Environmental Health Science and Engineering* **18** (2), 853–864.

Shao, P., Duan, X., Xu, J., Tian, J., Shi, W., Gao, S., Xu, M., Cui, F. & Wang, S. 2017 Heterogeneous activation of peroxymonosulfate by amorphous boron for degradation of bisphenol S. *Journal of Hazardous Materials* **322**, 532–539.

Sharma, M. & Vaish, R. 2021 Piezo/pyro/photo-catalysis activities in Ba0.85ca0.15(Ti0.9zr0.1)1-xfexo3 ceramics. *Journal of the American Ceramic Society* **104** (1), 45–56.

Singh, H., Chauhan, G., Jain, A. K. & Sharma, S. K. 2017 Adsorptive potential of agricultural wastes for removal of dyes from aqueous solutions. *Journal of Environmental Chemical Engineering* **5** (1), 122–135.

Soni, H. & Padmaja, P. 2014 Palm shell based activated carbon for removal of bisphenol A: an equilibrium, kinetic and thermodynamic study. *Journal of Porous Materials* **21** (3), 275–284.

Sotelo, J. L., Ovejero, G., Rodríguez, A., Álvarez, S. & García, J. 2013 Analysis and modeling of fixed bed column operations on flumequine removal onto activated carbon: PH influence and desorption studies. *Chemical Engineering Journal* **228**, 102–113.

Sudhaik, A., Raizada, P., Shandilya, P., Jeong, D. Y., Lim, J. H. & Singh, P. 2018 Review on fabrication of graphitic carbon nitride based efficient nanocomposites for photodegradation of aqueous phase organic pollutants. *Journal of Industrial and Engineering Chemistry* **67**, 28–51.

Sudhakar, P., Mall, I. D. & Srivastava, V. C. 2016 Adsorptive removal of bisphenol-A by rice husk ash and granular activated carbon – A comparative study. *Desalination and Water Treatment* **57** (26), 12375–12384.

Tagliavini, M., Engel, F., Weidler, P. G., Scherer, T. & Schäfer, A. I. 2017 Adsorption of steroid micropollutants on polymer-based spherical activated carbon (PBSAC). *Journal of Hazardous Materials* **337**, 126–137.

Tajik, S., Beitollahi, H., Nejad, F. G., Zhang, K., Van Le, Q., Jang, H. W., Kim, S. Y. & Shokouhimehr, M. 2020 Recent advances in electrochemical sensors and biosensors for detecting bisphenol A. *Sensors (Basel, Switzerland)* **20** (12), 1–18. /pmc/articles/PMC7349560/. (accessed 26 April 2023).

Tamjidi, S., Moghadas, B. K., Esmaeili, H., Shakerian Khoo, F., Gholami, G. & Ghasemi, M. 2021 Improving the surface properties of adsorbents by surfactants and their role in the removal of toxic metals from wastewater: a review study. *Process Safety and Environmental Protection* **148**, 775–795.

Tang, L., Xie, Z., Zeng, G., Dong, H., Fan, C., Zhou, Y., Wang, J., Deng, Y., Wang, J. & Wei, X. 2016 Removal of bisphenol A by iron nanoparticle-doped magnetic ordered mesoporous carbon. *RSC Advances* **6** (31), 25724–25732. Available from: https://pubs.rsc.org/en/content/articlehtml/2016/ra/c5ra27710h (accessed 2 May 2023).

Tang, Z., Peng, S., Hu, S. & Hong, S. 2017 Enhanced removal of bisphenol-AF by activated carbon-alginate beads with cetyltrimethyl ammonium bromide. *Journal of Colloid and Interface Science* **495**, 191–199. Available from: https://www.researchgate.net/publication/313230169_Enhanced_Removal_of_Bisphenol-AF_by_Activated_Carbon-Alginate_Beads_with_Cetyltrimethyl_Ammonium_Bromide (accessed 27 April 2023).

Thompson, R. C., Moore, C. J., Saal, F. S. V. & Swan, S. H. 2009 Plastics, the environment and human health: current consensus and future trends. *Philosophical Transactions of the Royal Society B: Biological Sciences* **364** (1526), 2153. /pmc/articles/PMC2873021/. (accessed 25 April 2023).

Tzatzarakis, M. N., Karzi, V., Vakonaki, E., Goumenou, M., Kavvalakis, M., Stivaktakis, P., Tsitsimpikou, C., Tsakiris, I., Rizos, A. K. & Tsatsakis, A. M. 2017 Bisphenol A in soft drinks and canned foods and data evaluation. *Food Additives & Contaminants: Part B* **10** (2), 85–90.

Vakili, M., Rafatullah, M., Salamatinia, B., Ibrahim, M. H., Ismail, N. & Abdullah, A. Z. 2017 Adsorption studies of methyl tert-butyl ether from environment. *Separation and Purification Reviews* **46** (4), 273–290.

Vasiljevic, T. & Harner, T. 2021 Bisphenol A and its analogues in outdoor and indoor air: properties, sources and global levels. *Science of the Total Environment* **789**, 1–16.

Vidovix, T. B., Januário, E. F. D., Bergamasco, R. & Vieira, A. M. S. 2021 Bisfenol A adsorption using a low-cost adsorbent prepared from residues of babassu coconut peels. *Environmental Technology (United Kingdom)* **42** (15), 2372–2384.

Wang, G., Wu, F., Zhang, X., Luo, M. & Deng, N. 2006 Enhanced TiO2 photocatalytic degradation of bisphenol E by β-cyclodextrin in suspended solutions. *Journal of Hazardous Materials* **133** (1–3), 85–91.

Wang, C. C., Du, X. D., Li, J., Guo, X. X., Wang, P. & Zhang, J. 2016 Photocatalytic Cr(VI) reduction in metal-organic frameworks: a mini-review. *Applied Catalysis B: Environmental* **193**, 198–216.

Wang, H., Liu, Z. H., Zhang, J., Huang, R. P., Yin, H., Dang, Z., Wu, P. X. & Liu, Y. 2019 Insights into removal mechanisms of bisphenol A and its analogues in municipal wastewater treatment plants. *Science of the Total Environment* **692**, 107–116.

Wang, J., Zhang, X., Li, Z., Ma, Y. & Ma, L. 2020 Recent progress of biomass-derived carbon materials for supercapacitors. *Journal of Power Sources* **451**, 1–17.

Wang, T., Xue, L., Zheng, L., Bao, S., Liu, Y., Fang, T. & Xing, B. 2021 Biomass-derived N/S dual-doped hierarchically porous carbon material as effective adsorbent for the removal of bisphenol F and bisphenol S. *Journal of Hazardous Materials* **416**, 1–25.

Wang, Z., Li, Q., Su, R., Lv, G., Wang, Z., Gao, B. & Zhou, W. 2022 Enhanced degradation of bisphenol F in a porphyrin-MOF based visible-light system under high salinity conditions. *Chemical Engineering Journal* **428**, 132106.

Wirasnita, R., Hadibarata, T., Yusoff, A. R. M. & Yusop, Z. 2014 Removal of bisphenol a from aqueous solution by activated carbon derived from oil palm empty fruit bunch. *Water, Air, and Soil Pollution* **225** (10). Available from: https://www.researchgate.net/publication/266477464_Removal_of_Bisphenol_A_from_Aqueous_Solution_by_Activated_Carbon_Derived_from_Oil_Palm_Empty_Fruit_Bunch (accessed 28 April 2023).

Wirasnita, R., Mori, K. & Toyama, T. 2018 Effect of activated carbon on removal of four phenolic endocrine-disrupting compounds, bisphenol A, bisphenol F, bisphenol S, and 4-tert-butylphenol in constructed wetlands. *Chemosphere* **210**, 717–725.

Wu, F. C., Tseng, R. L. & Juang, R. S. 2009 Characteristics of Elovich equation used for the analysis of adsorption kinetics in dye-chitosan systems. *Chemical Engineering Journal* **150** (2–3), 366–373.

Wu, L. H., Zhang, X. M., Wang, F., Gao, C. J., Chen, D., Palumbo, J. R., Guo, Y. & Zeng, E. Y. 2018 Occurrence of bisphenol S in the environment and implications for human exposure: a short review. *Science of the Total Environment* **615**, 87–98.

Wu, S., Liu, H., Yang, C., Li, X., Lin, Y., Yin, K., Sun, J., Teng, Q., Du, C. & Zhong, Y. 2020 High-performance porous carbon catalysts doped by iron and nitrogen for degradation of bisphenol F via peroxymonosulfate activation. *Chemical Engineering Journal* **392**, 1–47.

Xu, J., Lv, H., Yang, S. T. & Luo, J. 2013 Preparation of graphene adsorbents and their applications in water purification. *Reviews in Inorganic Chemistry* **33** (2–3), 139–160.

Xu, Y., Lin, W., Wang, H., Guo, J., Yuan, D., Bao, J., Sun, S., Zhao, W. & Zhao, C. 2020 Dual-functional polyethersulfone composite nanofibrous membranes with synergistic adsorption and photocatalytic degradation for organic dyes. *Composites Science and Technology* **199**, 1–10.

Yang, Y., Guan, J., Yin, J., Shao, B. & Li, H. 2014 Urinary levels of bisphenol analogues in residents living near a manufacturing plant in south China. *Chemosphere* **112**, 481–486.

Yousif, E. & Haddad, R. 2013 Photodegradation and photostabilization of polymers, especially polystyrene: review. *SpringerPlus* **2** (1), 1–32.

Yuan, L., Qi, M. Y., Tang, Z. R. & Xu, Y. J. 2021 Coupling strategy for CO_2 valorization integrated with organic synthesis by heterogeneous photocatalysis. *Angewandte Chemie – International Edition* **60** (39), 21150–21172.

Zafar, S., Mirza, M. L., Khalid, N. & Daud, M. 2015 Kinetic studies of the adsorption of thorium ions onto rice husk from aqueous media: linear and nonlinear approach. *Nucleus (Islamabad)* **52** (1), 14–19. Available from: http://inis.iaea.org/Search/search.aspx?orig_q=RN:47083040 (accessed 2 May 2023).

Zaib, Q., Khan, I. A., Saleh, N. B., Flora, J. R. V., Park, Y. G. & Yoon, Y. 2012 Removal of bisphenol a and 17β-estradiol by single-walled carbon nanotubes in aqueous solution: adsorption and molecular modeling. *Water, Air, and Soil Pollution* **223** (6), 3281–3293.

Zango, Z. U., Jumbri, K., Sambudi, N. S., Ramli, A., Bakar, N. H. H. A., Saad, B., Rozaini, M. N. H., Isiyaka, H. A., Jagaba, A. H., Aldaghri, O. & Sulieman, A. 2020 A critical review on metal-organic frameworks and their composites as advanced materials for adsorption and photocatalytic degradation of emerging organic pollutants from wastewater. *Polymers* **12** (11), 2648. Available from: https://www.mdpi.com/2073-4360/12/11/2648/htm (accessed 28 April 2023).

Zhai, Z., Ren, K., Zheng, X., Chen, Y., Dong, Y. & Shi, H. 2022 Simultaneous photocatalytic tetracycline oxidation and chromate reduction via a jointed synchronous pathway upon Z-scheme Bi12O17Cl2/AgBr: insight into intermediates and mechanism. *Environmental Science: Nano* **9** (5), 1780–1793. Available from: https://pubs.rsc.org/en/content/articlehtml/2022/en/d2en00028h (accessed 27 April 2023).

Zhang, Y. & Chu, W. 2022 Bisphenol S degradation via persulfate activation under UV-LED using mixed catalysts: synergistic effect of Cu–TiO2 and Zn–TiO2 for catalysis. *Chemosphere* **286**, 131797.

Zhang, L., Pan, F., Liu, X., Yang, L., Jiang, X., Yang, J. & Shi, W. 2013 Multi-walled carbon nanotubes as sorbent for recovery of endocrine disrupting compound-bisphenol F from wastewater. *Chemical Engineering Journal* **218**, 238–246.

Zhang, Y., Cheng, Y., Chen, N., Zhou, Y., Li, B., Gu, W., Shi, X. & Xian, Y. 2014 Recyclable removal of bisphenol A from aqueous solution by reduced graphene oxide-magnetic nanoparticles: adsorption and desorption. *Journal of Colloid and Interface Science* **421**, 85–92. Available from: https://pubmed.ncbi.nlm.nih.gov/24594036/ (accessed 27 April 2023).

Zhang, Y., Cui, W., An, W., Liu, L., Liang, Y. & Zhu, Y. 2018 Combination of photoelectrocatalysis and adsorption for removal of bisphenol A over TiO2-graphene hydrogel with 3D network structure. *Applied Catalysis B: Environmental* **221**, 36–46.

Zhang, Y., Zhao, M., Cheng, Q., Wang, C., Li, H., Han, X., Fan, Z., Su, G., Pan, D. & Li, Z. 2021 Research progress of adsorption and removal of heavy metals by chitosan and its derivatives: a review. *Chemosphere* **279**. Available from: https://www.researchgate.net/publication/351645248_Research_progress_of_adsorption_and_removal_of_heavy_metals_by_chitosan_and_its_derivatives_A_review (accessed 3 July 2023).

Zhao, C., Wang, Y., Zhao, R. & Jiang, J. 2022 Removal of bisphenol S from drinking water by adsorption using activated carbon and the mechanisms involved. *International Journal of Environmental Science and Technology* **19** (6), 5289–5300.

Zheng, S., Sun, Z., Park, Y., Ayoko, G. A. & Frost, R. L. 2013 Removal of bisphenol A from wastewater by Ca-montmorillonite modified with selected surfactants. *Chemical Engineering Journal* **234**, 416–422.

Zhou, Y., Chen, L., Lu, P., Tang, X. & Lu, J. 2011 Removal of bisphenol A from aqueous solution using modified fibric peat as a novel biosorbent. *Separation and Purification Technology* **81** (2), 184–190.

Zhou, M., Wu, Y. N., Qiao, J., Zhang, J., McDonald, A., Li, G. & Li, F. 2013 The removal of bisphenol A from aqueous solutions by MIL-53(Al) and mesostructured MIL-53(Al). *Journal of Colloid and Interface Science* **405**, 157–163.

Zhu, H., Li, Z. & Yang, J. 2018 A novel composite hydrogel for adsorption and photocatalytic degradation of bisphenol A by visible light irradiation. *Chemical Engineering Journal* **334**, 1679–1690.

First received 10 May 2023; accepted in revised form 21 August 2023. Available online 1 September 2023